

UC San Diego

UC San Diego Electronic Theses and Dissertations

Title

Elucidating Dynamic Interactions of Neuroligin4 with Alpha and [Beta]-Neurexin1 via Deuterium Exchange Mass Spectrometry /

Permalink

<https://escholarship.org/uc/item/9j5227dm>

Author

Lee, David Eugene

Publication Date

2013

Peer reviewed|Thesis/dissertation

UNIVERSITY OF CALIFORNIA, SAN DIEGO

Elucidating Dynamic Interactions of Neuroligin4 with Alpha and Beta-Neurexin1 via
Deuterium Exchange Mass Spectrometry

A Thesis submitted in partial satisfaction of the requirements for the degree
Master of Science

in

Biology

by

David Eugene Lee

Committee in charge:

Professor Palmer Taylor, Chair
Professor Darwin Berg, Co-Chair
Professor Darren Casteel
Professor Shelley Halpain

2013

The Thesis of David Eugene Lee is approved and it is acceptable in quality and form for publication on microfilm and electronically:

Co-Chair

Chair

University of California, San Diego

2013

DEDICATION

To my parents, Dean and Virginia, who provided the continued guidance and support I needed to make it this far and have yet to go.

To my brother Eric whose personality, intellect, and humor I relied on so much to help keep me balanced when things seemed to be losing control.

To my god-brother Mitchell for always being there when I could use a hand.

To my late mentor, Dr. Virgil Woods Jr., for pushing me to test my limits, holding me to the very high standards by which he himself lived by, and instilling in me a work ethic necessary to be a competent man of science.

EPIGRAPH

“Don’t wait until everything is just right. It will never be perfect. There will always be challenges, obstacles, and less than perfect conditions. So what? Get started now. With each step you take, you will grow stronger and stronger, more and more skilled, more and more self-confident, and more and more successful” – Mark Victor Hansen

TABLE OF CONTENTS

Signature Page	iii
Dedication	iv
Epigraph.....	v
Table of Contents	vi
List of Figures	vii
List of Tables	viii
Acknowledgements	ix
Abstract of the Thesis	xi
Introduction	1
Materials and Methods	13
Results	20
Discussion	30
Figures	37
Tables	83
References	86

LIST OF FIGURES

Figure 1: Three primary types of amino acid hydrogens	37
Figure 2: Hydrogen/Deuterium exchange rate in relation to pH	38
Figure 3: Schematic overview of deuterium exchange setup	39
Figure 4: Purity analysis of neuroligin4	40
Figure 5: Pepsin fragmentation map	41
Figure 6: Deuterium exchange profile for α -neurexin1	47
Figure 7: Deuterium difference maps for α -neurexin1	55
Figure 8: Deuterium exchange profile for β -neurexin1	61
Figure 9: Deuterium difference maps for β -neurexin1	67
Figure 10: Deuterium exchange profile for neuroligin4	71
Figure 11: Deuterium difference maps for neuroligin4	77

LIST OF TABLES

Table 1: Coverage statistics for α -neurexin1	83
Table 2: Coverage statistics for β -neurexin1	84
Table 3: Coverage statistics for neuroligin4	85

ACKNOWLEDGEMENTS

I wish to extend my gratitude first and foremost to Dr. Virgil Woods Jr. for entrusting me with carrying out this project and allowing me to have a role in making differences in people's lives. His reputation in proteomics brought me to his lab but it was more his sheer love of learning, teaching, and commitment to excellence which propelled me forward as a student. It is unfortunate that he was unable to see this work come to fruition but I hope that the contents of this manuscript would be quality enough for his standards so as to carry on his reputation and continue effecting change in this world.

My thanks also go to Dr. Palmer Taylor not only for being willing to fill in for Dr. Woods in a time of great need, but also for being so willing to share your knowledge and passion at the most crucial of times so that I would be able to keep moving forward.

Dr. Darwin Berg, Dr. Shelley Halpain, and Dr. Darren Casteel, each of you have my gratitude as well for being willing to set time aside to serve as my committee members.

To Meghan Miller, Davide Comoletti, and Jennifer Wilson, I thank each of you for your valuable contributions in helping move this project forward.

I would also like to thank Dr. Sheng Li and Dr. Tong Liu for the invaluable advice and assistance each provided as I progressed. This project would certainly have still been far from completion had it not been for your endless patience, candid feedback, and valuable advice.

Last but not least, my unwavering gratitude goes out to Brian Wong, Bryant Kou, Danny Tran, Daphne Wang, and Henry Guan for all of your intellectual input, moral

support, and of course, countless hours spent helping me manually sorting through data bit by bit.

The Introduction section, in part is currently being prepared for submission for publication of the material with the thesis author and coauthors Sheng Li and Palmer Taylor.

The Materials and Methods section, in part is currently being prepared for submission for publication of the material with the thesis author and coauthors Sheng Li and Palmer Taylor.

The Results section, in part is currently being prepared for submission for publication of the material the thesis author and coauthors Sheng Li and Palmer Taylor.

The Discussion section, in part is currently being prepared for submission for publication of the material the thesis author and coauthors Sheng Li and Palmer Taylor.

ABSTRACT OF THE THESIS

Elucidating Dynamic Interactions of Neuroligin4 with Alpha and Beta-Neurexin1 via
Deuterium Exchange Mass Spectrometry

by

David Eugene Lee

Master of Science in Biology

University of California, San Diego, 2013

Professor Palmer Taylor, Chair

Professor Darwin Berg, Co-Chair

Synaptic adhesion molecules such as neuroligins and neurexins play a critical role in nervous system development and aberrations in their structure appear associated with developmental conditions such as the Autism Spectrum Disorders. Yet why two distinct α - and β - neurexin protein isoforms emerged in the synapse is still not well understood. Neurexins are composed of either α - forms containing six distinct Laminin-Neurexin-Sex

(LNS 1-6) hormone binding globulin domains and three epidermal growth factor like domains (EGF 1-3), and β - forms which are solely composed of the sixth LNS domain. Both serve as presynaptic cell adhesion molecules and bind to postsynaptic neuroligins which are members of the α - β hydrolase fold family. It is hypothesized that though binding of neuroligin to neurexins is strongest at the sixth LNS domain, or β -neurexin, it may not have to occur there exclusively due to established variance in protein function.

Hydrogen/Deuterium Exchange Mass Spectrometry (DXMS) was utilized to elucidate structural components of neuroligin4 and α - and β -neurexin1 and probe for changes induced by binding interactions. This revealed in neuroligin a novel point of interaction with α -neurexin through reductions in deuterium exchange rates absent when bound to beta-neurexin1. α -neurexin1 exchange profiles also affirmed physical occlusion at LNS 4 and 5 yet neuroligin's binding site remained specific to LNS 6. Furthermore β -neurexin1 displayed binding trends highly similar to α -neurexin1's LNS 6 and confirmed both bind neuroligin4 in the same fashion and that potential neuroligin interaction with LNS 4 and 5 exert minimal effects on LNS 6 binding.

INTRODUCTION

Neuroigin and Neurexin: Partners of Synaptic Transmission

The α - β hydrolase fold superfamily of proteins are diverse in structure and function. Yet these tend to share common pathways for protein folding and processing. Not only do they serve as catalytic centers for substrate ester and amide hydrolysis as well as chaperones in thyroid hormone synthesis, they are responsible for maintaining neuronal communications through vital heterophilic synaptic adhesion interactions (De Jaco et al., 2012). The latter function is carried out through the binding of neurexin and neuroigin class cell adhesion proteins (Davletov et al., 2003; Dean et al., 2003; Fabrichny et al., 2007, Leone et al., 2010; Miller et al., 2011; Sudhof, 2001; Sudhof, 2008; Ushkaryov et al., 2008).

Vertebrates possess three distinct neurexin genes labeled neurexin 1-3, each of which can be transcribed to produce the longer α -neurexin or the shorter β -neurexin via alternative promoter regions (Leone et al., 2010; Miller et al., 2011). Translation of neurexin transcripts leads to the production of presynaptic class I transmembrane proteins whom all possess the same C-terminal sequence anchoring them to the cell. Their N-terminal regions, however, differ. α -Neurexin is comprised of nine distinct and independently folded domains which include six laminin-neurexin-sex hormone-binding globulin domains, or LNS domains, and three epidermal growth factor-like domains, or EGF domains. The C-terminal region is composed of an O-glycosylated stalk domain consisting of approximately 100 amino acids and functions as an elongated flexible linker to the protein's transmembrane domain. The setup varies between the two forms in that

the β form is solely composed of the last LNS domain of α -neurexin and lacks any EGF domains (Miller et al, 2011). These two forms are further diversified through five potential alternative splicing sites labeled SS#1-5 of which α -neurexin can utilize all five whereas β -neurexin only can access site 4 and 5. It is believed that different forms have a significant influence on synapse specificity (Comoletti et al. 2006; Ichtchenko et al., 1996; Ullrich et al., 1995).

Neuroligins are another family of class I transmembrane cell-adhesion proteins consisting of five main isoforms designated neuroligin 1-4 and 4Y. The proper selection of these isoforms which exhibit sequence homologies ranging from 32-36% plays a significant role in the proper maintenance of glutamatergic excitatory synapses which utilize neuroligins 1, 3, and 4 as well as GABAergic inhibitory synapses which utilize neuroligin 2 (Leone et al., 2010; Song et al., 1999; Varoqueaux et al., 2004). As postsynaptic cell adhesion proteins they interact and bind with neurexin class proteins to effectively convey neuronal signals via characteristic release of neuronal transmitter across the synaptic cleft. When induced to be expressed by non-neuronal cells they aid in the formation of functional presynaptic structures, which can then be connected to postsynaptic projection to initiate transmission (Brose et al., 1999; Garner et al., 2002). They are close relatives of cholinesterases, lipases, protein neurotactins, glutactins, gliotactins, and thyroglobulins which are also members of the α/β -hydrolase fold superfamily (Auld et al., 1995; Cygler et al., 1993; de la Escalera, 1990; Ollis et al., 1992; Olson et al., 1990; Schumacher et al., 1986) yet instead of utilizing its now-vestigial catalytic pocket to perform hydrolysis and transmit signal, it utilizes surface recognition properties to execute its role (Fabrichny et al., 2007).

The proper assembly, delivery, and placement of these two families of proteins should not be taken lightly. In studies both past and present there are been results associating complications with the proper formation of the neuroligin-neurexin complex with the onset of disorders such as ASD, Tourette's Syndrome, schizophrenia, as well as learning disabilities (Sudhof, 2008). Genetic screening has largely determined that mutations within the coding sequence whether they be deletions, truncations, or point mutations often do not necessarily affect the proper binding and formation of the complex but rather can drastically hinder the post-translational processing and delivering of protein to the target dendritic or axonal surface (Arons et al., 2012; Fabrichny et al., 2007; Jamain et al., 2003; Leone et al., 2010; Miller et al., 2011; Yan et al., 2008; Zhang et al., 2013). This has been determined to be a result of a protein's inability to properly fold and be glycosylated in lieu of any changes, thus leading to intracellular retention. For any that do manage to get out, they are quickly labeled for degradation and removed, further depriving the synapse of points of connectivity (De Jaco et al., 2012).

Given the role that neuroligin and neurexin play in synaptic transmission, the specifics surrounding their interactions have been well studied. The two families of proteins are capable of interacting with one another in a calcium dependent fashion where a single cation will coordinate assembly of the complex via its specific binding sites on either protein. Neuroligin forms a dimer with itself in antiparallel form along its four-helix bundle. This setup thus leaves two β -neurexin proteins to bind on opposite sides of the dimeric molecule through coordination with calcium in between their respective binding interfaces to neuroligin as shown via X-ray crystallography. (Arac et al., 2007; Chen et al., 2008; Fabrichny et al., 2007; Leone et al., 2010; Miller et al., 2011). On the

other hand whether calcium plays a role outside of coordinating complex formation, whether neuroligin4 binding to the LNS 6 region of α -neurexin1 is consistent with that of β -neurexin1, as well as why the latter may have evolved, are questions that have not been extensively examined. With multiple independently folding domains, where LNS 2 and LNS 6 domains have been shown to possess capacity for direct protein binding, curiosity regarding the roles played by the LNS 3-5 domains found in between inevitably rise as well (Sugita et al., 2001). In this paper we demonstrate that calcium coordination leads to protein stabilization, LNS 6 binding to neuroligin is not notably influenced by the presence of additional LNS domains, and LNS 4 and 5 domains may serve as points for additional stabilization and potential function of the bound complex through transient interactions with neuroligin.

Relation to Autism Spectrum Disorder

ASD has been linked to issues of protein structure of neuroligins as well as neurexins (Arons et al., 2012; Sudhof, 2001). They can also induce symptoms of schizophrenia, Pitt Hopkins-like syndrome 2 and mental retardation (Kim et al., 2008; Rujescu et al., 2009; Sebat et al., 2007; Yan et al., 2008; Zahir et al., 2008; Zweier et al., 2009). Some have hypothesized that these mutations likely either cause an issue with binding integrity or proper signaling either by neurotransmitter release or by some yet-to-be-determined metabolic product. Changes in one or more facets of synapse formation, maintenance, signaling, and plasticity have frequently been under scrutiny. Generally in cases where an individual suffers from disorders which prevents proper expression, delivery, or interaction with neuroligin, the condition renders an effective loss-of-

function of neuroligin and subsequently induces a mismatch between the balance of excitatory to inhibitory networks functioning at any given point in time (Dean et al., 2003; Sudhof, 2008; Yan et al., 2008; Zhang et al., 2009).

The genetic basis for such is a complex one and has yet to be fully understood. For example it has proposed an interaction with protein SHANK3 where levels of expression had a close correlation to the rate of excitatory synapse formation which leads to increases in neuroligin levels. Upregulation of such promotes the proliferation of excitatory synapses but does not fully establish an explanation for its role in how it contributes to proper synapse maturation (Arons et al., 2012). Other studies have localized points of interest to particular X-linked genes which may affect proper protein folding, binding, or post-translational modification through variance of number of gene copies, physical alterations of chromosomes, specific sequence mutations along with missense mutations (Jamain et al., 2003; Feng et al., 2006; Glessner et al., 2009; Kim et al., 2008; Rujescu et al., 2009; Sebat et al., 2007; Szatmari et al., 2007; Yan et al., 2008; Zahir et al., 2008; Zweier et al., 2009). These changes that affect neuroligin's structural, function, and availability provide us with a look at how far we have come and how much more there is to be done to fully comprehend it.

The neurexin family which is involved with presynaptic neuroligin binding is not excluded from these considerations. Since synaptic signaling is a concerted effort by both neuroligin and neurexin, loss of the latter can be just as problematic as issues with the former. α -Neurexins have been shown to not only participate in binding with neuroligin to connect a bridge for signaling, but they are also responsible for regulating proper function of synaptic calcium channels (Missler et al, 2003). Changes in its

structure lead to an inability to properly couple signals with calcium channel opening and as a result effectively interfere with transmissions which likely lead to a diminished neuronal response (Schapitz et al., 2010). Even while synapses might contain a functional copy of β -neurexin, it is unable to compensate effectively for the roles that α -neurexin fills, accordingly the question of what α -neurexin's full spectrum of functions are have yet to be completely answered (Sudhof, 2008). Seeing as how evidence towards linking the formation of the neuroligin-neurexin adhesion complex and the linkage to ASD via mutations in synaptic adhesion proteins still remains fairly incomplete, it would be of interest to further elucidate the fundamental mechanisms of cell-to-cell adhesion to isolate whether these observed complications are solely due to independent causes or a culmination of a series of related symptoms.

Background surrounding Hydrogen/Deuterium Exchange Mass Spectrometry

With a seemingly ever increasing list of health issues that may impact an individual's ability to experience an otherwise fulfilling life, there must be a comprehensive understanding of protein structure, function, and conformational dynamics to define the targets of novel treatments. With each protein possessing its own biological and physical characteristics, the task of quickly and efficiently cataloging all pertinent information on the protein's properties can be a very difficult and highly time consuming one. However with the development of modern techniques such as X-ray crystallography and surface plasmon resonance, proteins have become far easier to observe, assess, and isolate for experimentation. Even so, significant hurdles still remain

in that each technique usually can only provide a limited scope of information on each protein (Wintrode et al., 2007).

Peptide amide hydrogen/deuterium exchange mass spectrometry, or more commonly referred to as DXMS, has become one of the most frequently utilized tools in analysis of protein dynamic interactions. It serves as a method to rapidly and efficiently map out binding footprints in protein-protein or protein-antigen type interactions. Utilizing this technique provides a wider perspective than possible through function of point mutants alone. Prior to deuterium exchange, hydrogen exchange studies were and still are performed using proton NMR (Chandak et al., 2013; Dyson et al., 2004). Nowadays mass spectrometry has come to be viewed as a highly preferable choice for protein hydrogen-exchange experiments (Chung et al 2011, Kaltashov et al., 2002; Westfield et al., 2011). DXMS itself is also viewed as an advantageous technique in comparison to others in that the amount of protein needed to perform an experiment is significantly less than traditional methods (400-1500 picomoles), and it makes elucidation of protein structure possible even if crystallization is not possible, since analysis of protein is conducted directly in solution (Maier et al., 2005; Morgan et al., 2009). Like what can be said about most organic molecules, a protein's unique structure and conformational dynamics are determinants of its functionality. Any alterations to said structure either through amino acid mutation or changes in post translational modifications can drastically influence protein function. By applying DXMS to interests in disease progression, DXMS has allowed for the tracking of shifts in protein structure and function in comparison to wild-type counterparts. Since its inception it has also been of great use in observing dynamic interactions and structures of various proteins related

to human diseases such as those found in aggressive neurodegenerative disease, platelet activation, and viral infections (Hsu et al., 2009; Lee et al., 2011; Zhang et al., 2012, Aiyegbo et al., 2013). In this study, DXMS is applied to neuroligin4, α -neurexin1, and β -neurexin1, which when functioning abnormally have been shown to be related to, amongst other complications, onset of Autism Spectrum Disorders (ASD), Tourette's Syndrome, schizophrenia, and learning disabilities (Sudhof, 2008).

Theory behind Hydrogen/Deuterium Exchange

The phenomenon of hydrogen exchange occurs more often than most individuals realize. It is characterized by the deprotonation of a hydrogen from an atom in the molecule being studied along with subsequent reprotonation by a hydrogen from solution. Hydrogens on proteins are largely categorized into three groups. The first consists of those which make up general hydrocarbons which fail to exhibit any measurable levels of exchange. The second contains functional groups found on amino acids (-COOH, -NH₂, -SH, -OH) where exchange occurs too rapidly and cannot be accurately measured due to the majority of deuterium having back exchanged with solution during mass spectrometry processing. Finally the third group is made up of peptidic backbone hydrogens which display appreciable rates of exchange due to stabilization of surrounding amide groups. DXMS utilizes this property to track rates of hydrogen exchange and can examine all amino acids with the exception of proline which lacks an amide hydrogen on the peptidic backbone (Figure 1). When under physiological conditions, peptidic amide hydrogens have exchange rates varying from a few milliseconds to hours, days, or in some instances

even weeks due to influences of inherent protein structure and regional solvent accessibility (Morgan et al., 2009).

Peptidic amide hydrogens are known to be weakly acidic and can normally exchange with hydrogens in solution without any trace of such activity. If however the solvent hydrogen is replaced with a heavier isotope such as deuterium, mass spectrometry can precisely identify locations where exchange-induced mass increase has occurred. The overall rate of hydrogen-deuterium exchange across a protein is largely determined by its structural conformation and solvent accessibility and can be further influenced by binding interactions (Englander and Kallenbach., 1983). That means areas of proteins which are structurally organized or sterically impeded by physical obstruction show a lesser degree of hydrogen exchange whereas areas that generally lack structure or possess greater degrees of mobility exhibit much more rapid rates of exchange (Bai et al., 1993; Garcia et al., 2005). Thus with having collected such information, valuable contributions can be made to existing as well as novel understandings of proteins interacting under physiological conditions.

The rate of amide hydrogen exchange as mentioned above can shift as additional considerations are made for local factors such as steric hindrance by neighboring side chains in key solvent causeways or by binding of organic molecules such as ligands or antibodies which can potentially physically occlude various areas upon occupation. Hydrogen exchange takes place when a solvent base physically deprotonates a peptidic hydrogen and a deuterated solvent molecule comes in to replace the lost proton (Englander et al., 1996). Anything that impedes this can severely inhibit efficient exchange. In functional native conformation proteins, any amide hydrogens located on

unstructured/variable loop regions or lacking any sort of additional stabilization by hydrogen bonding will usually display a very high degree of exchange on the scale of milliseconds to seconds. Peptidic hydrogens buried deep within a hydrophobic interior or perhaps involved in indispensable hydrogen bonding may take days, weeks or even months to see any appreciable degree of exchange (Tsutsui et al. 2007; Zhang and Smith., 1993). Similar trends are also observed once a binding partner has docked and hidden otherwise exposed areas of the target protein which can exhibit clear differences in exchange in comparison to its free counterparts. (Zhang et al., 2012) Thus analyzing the rates of peptidic hydrogen exchange can provide vital information on protein structural layouts under physiological conditions as well as potential conformational changes due to dynamic interactions with other macromolecules.

Analysis of Hydrogen/Deuterium Exchange by Mass Spectrometry

A given DXMS study is comprised to two major experimental parameters: digestion optimization and deuterium on-exchange. Digestion optimization is the process by which the most optimal conditions of proteolysis are determined. Factors which must be considered are the concentrations of denaturant applied, what conditions the experiment took place under, the arrangement and type(s) of protease columns used, as well as appropriate flow rate over said protease column(s). To assess the effectiveness of these conditions, non-deuterated protein samples are prepared and mixed with a series of quench buffers varying in concentration of denaturant salt guanidinium hydrochloride to neutralize any protein structure. In addition, the levels of TCEP added to the quench must also be considered to ensure appropriate reduction of any disulfide bonds present.

Once this step has been completed, the samples are then injected and flowed across a conjugated protease column to be proteolyzed into daughter peptides generally ranging between 4 to 30 amino acids in length. These peptides are then separated via gradient elution by reverse-phase liquid chromatography. During this process primary data-dependent MS1 profile mode scans for parent mass identification to identify the peptides generated as a result of proteolysis in each quench condition, and subsequently follows it up with a MS/MS scan to identify the peptide sequence of daughter fragment ions. Upon completion of data acquisition, Proteome Discoverer, which is a program that utilizes a database search algorithm, is used to analyze the data and assigns further identifications of parent peptides including their sequence and chromatographic retention times for additional data reduction procedures. The optimal quench condition is one that ideally yields the greatest coverage of the protein's amino acid sequence and highest number of peptides, and will be used further to conduct deuterium on-exchange experiments.

Deuterium exchange experiments utilize the acidic nature of peptide bonds to incorporate isotopic deuterium labels onto a protein's peptidic backbone. A deuterium on-exchange experiment is performed so that the degree of deuteration across various portions of the protein can be assessed. This is done by comparing the levels of deuteration on a protein incubating in D₂O buffer over pre-determined time points versus that of protein incubating in H₂O buffer, both of which are occurring at each individual protein's native physiological conditions. The time points are pre-set incubation times where once time is up, an aliquot of the exchanging solution is "quenched" via mixing with quench solution and the temperature of the solution is cooled to 0°C. The quench functions to remove protein structure so as to allow proteases to function more effectively

as well as lower the solution pH to 2.5 so as to push acid/base catalyzed exchange reaction rates to a minimum which is not so important in preventing further deuterium labeling as it is in hindering loss of peptide deuterium to surrounding H₂O in solution (Figure 2). Thus quenching the solution at pH 2.5 maximizes deuterium retention and allows for the labeled peptides to be analyzed by mass spectrometry and peptide identification using the aforementioned procedures above. Once data acquisition of these experiments has been completed complete, the masses of the deuterated peptides can be compared and contrasted to the masses of their fellow non-deuterated counterparts. At the conclusion of data comparison, the peptides comprising these data sets can be used to construct a detailed map to quantitatively illustrate the varying rates of deuterium incorporation across different sectors of the protein over time. Thus generating such allows for the elucidation of structural dynamics across particular regions of interest as well as verifying domains for ligand or substrate interaction (Figure 3).

Acknowledgement

The Introduction section, in part is currently being prepared for submission for publication of the material with the thesis author and coauthors Sheng Li and Palmer Taylor.

MATERIALS AND METHODS

Neuroigin4 and A/B Neurexin1 Expression and Purification

Rat Neuroigin4 and bovine α -neurexin1 were expressed in HEK293 GnT1 mammalian cell lines via p-cDNA 3.1 with a 3Cpro cleavage site introduced upstream from the Fc domain as previously described (Bolliger et al., 2001; Comoletti et al., 2010; Miller et al., 2011; Ushkaryov et al., 1992) and rat β -neurexin1 was expressed in bacterial Rosetta Plys cells where initial pGEX construct (Comoletti et al., 2003; Comoletti et al., 2004, Ushkaryov et al., 1994) was subcloned into pDEST 17 (Invitrogen). These were then purified via immobilized anti-FLAG M2 antibody (Sigma Aldrich) and gel-filtration FPLC on Superdex 200 in buffer A as previously described. Stock solutions came out to 6.0 mg/ml, 5.3 mg/ml, 5.1 mg/ml respectively. Neuroigin stock was stored at 0°C while α - and β -neurexin stocks were divided into 100 ul aliquots and stored at -80°C. All reagents used for experimentation were at purities that were reagent grade at minimum.

Establishing Optimal Proteolysis Conditions

Before performing deuteration studies, quench conditions that could yield an optimal pepsin fragmentation pattern were identified. Five main conditions were attempted where stock concentration of guanidinium chloride was either 0.08M, 0.8M, 1.8M, 3.2M, or 6.4M. All of these also contained 15mM TCEP, 0.8% formic acid, and 16.6% glycerol. An additional condition containing 6.4M guanidinium chloride, 1M TCEP, 0.8% formic acid, 16.6% glycerol was also attempted. For Neuroigin with and without calcium (6.0 mg/ml stock solution), Neuroigin- α -Neurexin complex (4.5 mg/ml

stock solution) and Neuroligin- β -Neurexin complex (4.9 mg/ml stock solution), fragmentation study was performed by mixing 1.5 μ l of neuroligin stock solution suspended in 10 mM HEPES, 150 mM NaCl at pH 7.4 with 22.5 μ l of H₂O buffer (8.3 mM Tris, 150 mM NaCl in H₂O, pH 7.2), and subsequently aliquoted into 36 μ l of quench at 0°C. After allowing it to equilibrate for 60 s, autosampler vials were filled with 20 μ l aliquots and frozen at -80°C.

One last condition attempted followed similar to the preparation above where fragmentation study was performed by mixing 1.5 μ l of neuroligin stock solution suspended in 10 mM HEPES, 150 mM NaCl at pH 7.4 with 10.5 μ l of H₂O buffer (8.3 mM Tris, 150 mM NaCl in H₂O, pH 7.2), and subsequently aliquoted into 18 μ l of select quench and allowed to equilibrate for 300 s at 0°C. Thirty μ l of diluent (0 M GuHCl, 0.8% formic acid, 16.6% glycerol) were subsequently added and allowed to equilibrate for 60 s at 0°C. Samples were then aliquoted in 20 μ l amounts into autosampler vials and frozen at -80°C. A similar procedure was repeated in preparing α -Neurexin and β -Neurexin fragmentation studies.

Once ready for data acquisition samples were thawed at 5°C and flowed over an AL-20-pepsin column (16 μ l bed volume (Sigma)) packed with porcine pepsin (3,200-4,500 units/mg protein, St. Louis MO) coupled to Poros AL-20 μ m resin (Life Technologies, Grand Island, NY) at 30 mg protease/ml resin per manufacturer's instructions at a rate of 20 μ l/min. The resulting peptides were then collected onto a C18 trap column at 0°C (Michrom MAGIC C18AQ 0.2x2 mm) and separated via elution using a C18 reverse phase column at 0°C (Michrom MAGIC C18AQ 0.2x50 mm) utilizing a linear gradient of 8-48% solvent B (80% acetonitrile and 0.01% TFA) over 30

minutes with column effluent directed into an Orbitrap Elite mass spectrometer (ThermoFisher Scientific Orbitrap Elite). The instrument was set to operate in positive ESI mode with a sheath gas flow of 8 units, a spray voltage of 4.5 kV, a capillary temperature of 200°C, and an S-lens RF of 67%. Data acquisition was completed in both data dependent MS1:MS2 mode and MS1 profile mode (Zhang et al., 2012). Survey scan resolution was set to 60,000, at m/z 400 with a target value of 1×10^6 ions and 3 microscans. Maximal injection time for MS/MS fragmentation was varied between 25 and 200 ms. Dynamic exclusion was 30 s and early expiration was disabled. MS/MS fragmentation isolation window was set to 2, and the five most abundant ions were selected for product ion analysis. Resulting data utilized Proteome Discoverer SEQUEST software (ThermoFisher Scientific Inc.) to identify the sequence of peptide ions. Centroid scores of isotopic envelopes of nondeuterated, functionally deuterated, and equilibrium deuterated peptides were then assessed using DXMS Explorer (Sierra Analytics Inc, Modesto, CA) and subsequently converted to corresponding deuteration levels (Spraggon et al., 2004).

Preparation for Protein Deuteration On-Exchange Experimentation

To perform functional deuteration studies, the aqueous phase utilizes deuterated water obtained from Cambridge Isotope Laboratories (Andover, MA) which results in a 1 Dalton increase in the mass of a particular exchanged amide proton on a defined peptide. Deuterated water added to protein is buffered at physiological pH and ionic concentration. Over predetermined periods of time, as the protein becomes more labeled, aliquots of exchanged solution are quenched to drop the pH to 2.7, have disulfide bonds

reduced using tris (2-carboxyethyl) phosphine hydrochloride (TCEP) from Sigma (St. Louis, MO), and immersed in crushed dry ice to markedly reduce the rate of further exchange as well as deuterium label loss from the protein. The locations and amounts of deuterium exchange can be quantified after rapid protein denaturation and disulfide bond reduction, as well as digestion over solid phase pepsin. The shifts in mass of the resulting peptides induced by deuteration are detected via liquid chromatography mass spectrometry.

In preparation for deuterium exchange, neuroligin was prepared under four conditions either being calcium-deficient, calcium-bound, and in complex with either α -neurexin1 or β -neurexin1 with three states each: non-deuterated (ND), partially deuterated (PD), and equilibrium deuterated (FD). For calcium-deficient, 20 ul of neuroligin was diluted with 4.5 ul H₂O buffer (8.3 mM Tris, 150 mM NaCl in H₂O, pH 7.2) and 0.5ul EDTA at 25°C. For calcium-bound, 20 ul of neuroligin was diluted with 5 ul calcium-enriched H₂O buffer (8.3 mM Tris, 150 mM NaCl, 15mM Ca²⁺ in H₂O, pH 7.2) at 25°C to generate a working stock. α -Neurexin and β -neurexin were also incubated individually in calcium-enriched H₂O buffer. After 300 s incubation, neuroligin was mixed with α -neurexin and β -neurexin respectively in individual tubes at a 1:1.2 neuroligin:neurexin mole ratio and allowed 300 s to bind at 25°C.

For functional deuteration studies of calcium-bound neuroligin, 6.0 ul of working stock protein was mixed with 6.0 ul of calcium-supplemented H₂O buffer (8.3 mM Tris, 150 mM NaCl, 3mM Ca²⁺ in H₂O, pH 7.2) and then diluted into 36ul of calcium-supplemented D₂O buffer (8.3 mM Tris, 150 mM NaCl, 3mM Ca²⁺ in D₂O, pD_{read} 7.2) at 25°C. At 10 s, 100 s, 1000 s, 10,000 s, and 100,000 s, an 8 ul aliquot of the exchanging

solution was quenched via addition to 12 ul of optimized quench (6.4 M GuHCl, 1 M TCEP, 0.8% formic acid, 16.6% glycerol) chilled to 0°C on melting ice, allowed to equilibrate for 300 s, and diluted with 20 ul of diluent (0 M GuHCl, 0.8% formic acid, 16.6% glycerol) at 0°C which was subsequently allowed 60 s to equilibrate before transfer into autosampler vials in 20 ul aliquots. Vials were then immediately immersed in crushed dry ice and frozen at -80°C.

Nondeuterated samples were prepared by mixing 2 ul of neuroigin working stock solution with 14 ul of calcium-supplemented H₂O buffer (8.3 mM Tris, 150 mM NaCl, 3mM Ca²⁺ in H₂O, pH 7.2), and subsequently aliquoted into 24ul of optimized quench and allowed to equilibrate for 300 s at 0°C. 40 ul diluent containing 0 M GuHCl, 0.8% formic acid, 16.6% glycerol, was subsequently added and allowed to equilibrate for 60 s at 0°C. Samples were then aliquoted in 20 ul amounts into autosampler vials and frozen at -80°C.

Equilibrium deuterated samples were prepared by mixing 2 ul of neuroigin working stock solution with 2 ul of calcium-supplemented H₂O buffer (8.3 mM Tris, 150 mM NaCl, 3mM Ca²⁺ in H₂O, pH 7.2). 12 ul D₂O buffer containing 100% D₂O, 0.8% formic acid was added and the sample was left to incubate for 72 hours at 25°C. A 12 ul aliquot of exchanging sample was subsequently transferred into 18ul of optimized quench and allowed to equilibrate for 300 s at 0°C. Thirty ul of diluent were subsequently added and allowed to equilibrate for 60 s at 0°C. Samples were then aliquoted in 20 ul amounts into autosampler vials and frozen at -80°C. Data acquisition for each set of samples was completed in 8-hour blocks and acquired with MS1 profile analysis mode. The resulting data reduction was done via DXMS data reduction software described below. Studies of

α -neurexin and β -neurexin and respective complexes were completed similarly. For the α -neurexin study, an additional mole ratio of 1:3 was prepared and analyzed.

DXMS Data Processing

To assess the anticipated sequence of parent peptide ions from the large quantity of MS/MS data acquired from the mass spectrometer, Proteome Discoverer which was developed in collaboration with ThermoFischer Scientific Inc, Fairlawn, NJ, was utilized to assign initial peptide identifications. The program is a highly specialized DXMS-specific data reduction algorithm software which pooled all generated peptides and passed them through a primary quality control threshold which can be adjusted by the user. Each individual unique peptide was evaluated for accuracy and quality of the mass to envelope signal of the mass spectrum which was fitted along with the calculated mass envelope for further data reduction. Should a given peptide contain several charged residues, then the ionization states which possessed the highest signal-to-noise ratio was selected. In general circumstances the peptides which possessed the lowest charge states yielded the closest matches and optimally accurate signals.

Data processing is also needed to accommodate for “back-exchange” phenomena, characterized as the loss of deuterium from peptides into solution during processing and mass spectrometer analysis. This resulted from the presence of H₂O in the protein’s surroundings in addition to H₂O which could be found in the flow solvent carrying protein towards the mass spectrometer and protein’s innate ability to exchange with such molecules. Corrections for “back-exchange” of deuterium to hydrogen during processing were made through the following two equations developed by Zhang and Smith., 1993,

and allowed for the determination of more accurate levels of deuterium incorporation for each given peptide.

$$\text{Deuteration Level (\%)} = \frac{m(\text{P}) - m(\text{N})}{m(\text{F}) - m(\text{N})} \times 100$$

$$\text{Deuterium Incorporation (number)} = \frac{m(\text{P}) - m(\text{N})}{m(\text{F}) - m(\text{N})} \times \text{MaxD}$$

In each of the equations, $m(\text{N})$, $m(\text{P})$, and $m(\text{F})$ represent the centroid values assigned for non-deuterated, partially deuterated, and fully deuterated peptides respectively. MaxD is defined as the maximum value of deuterium which can be incorporated onto a given peptide. It can be calculated by from the total number of non-proline amino acids in a given peptide by subtracting the sum number of proline residues that are not found in the first two amino acid residues, along with an additional two to accommodate for the back-exchange rate of the first two N-terminal residues being too fast to allow for any appreciable measuring of deuteration levels.

Acknowledgement

The Materials and Methods section, in part is currently being prepared for submission for publication of the material with the thesis author and coauthors Sheng Li and Palmer Taylor.

RESULTS

Characterization of Neuroligin and Neurexin

Preparations of Neuroligin and Neurexins were quantified to have a purity of ~95% by coomassie (Figure 4). Neurexins were expressed to not contain splice site #4. In addition β -neurexin1 did not possess any glycosylation due to expression in bacterial cells incapable of attaching carbohydrate to β -neurexin1.

Fragmentation Optimization of Neuroligin4 and A-Neurexin1 and B-Neurexin1

Prior to initiating deuterium exchange experiments, we conducted fragmentation analysis to ascertain which set of quench conditions would yield optimal recovery of identifiable unique peptides on all three proteins separately and in complex with their respective partner(s). Quench conditions were defined by varying the concentration of guanidinium chloride and TCEP in each set of solutions. Ideally the condition chosen maximizes the number of overlapping peptides available and which together span the entire amino acid sequence of each respective protein. The results of the optimal experiment came out to be the quench solution containing high guanidinium chloride and TCEP (6.4 M and 1M respectively) followed by dilution (0 M guanidinium) prior to freezing. Proteolysis results for the three proteins across the pepsin column are shown in Table 1. For neuroligin4 and α -neurexin1 there are characteristic gaps due to N-linked glycosylations, while β -neurexin did not have any. For neuroligin they are found on Asn102 & Asn511 and α -neurexin on Asn813 and Asn1246. Furthermore for α -neurexin the EGF-3 region which is a cysteine-rich area is known to contribute to

disulfide bonding contains little to no coverage. Even so, none of the other quench conditions provided superior coverage, number of peptides, or both (data not shown). Therefore we selected this particular condition to conduct deuterium exchange experimentation as follows.

Analysis of Hydrogen/Deuterium Exchange

In order to characterize the conformation profile of each protein alone and in bound form, multiple conditions were developed to monitor the progressive change in deuteration. For each protein we used three standard conditions: calcium deficient, calcium bound, and in complex in a 1:1.2 ratio of target:partner protein. For α -neurexin, an additional ratio condition of 1:3 was also completed. For each set, protein was incubated in deuterated buffer for five set time points, quenching time points exchanging at 25°C from 10 s to 100,000 s with optimized quench chilled to 0°C on melting ice to drop the rate of back-exchange to a minimum as it underwent mass spectrometer analysis. In addition, we prepared non-deuterated and equilibrium-deuterated sets for each sample as negative and positive controls. With these the overall levels of deuterium incorporation in each set and time point was quantified via mass spectrometry and assigned a percent deuteration as detailed in the Materials and Methods section. To establish a proper deuteration profile, a peptide of specific length and charge state must be identified in the non-deuterated, functionally-deuterated, and equilibrium-deuterated conditions. As a result of experimental variation, there was inevitably some loss of peptides yielded which may or may not have resulted in coverage gaps not previously observed in initial fragmentation optimization experiments as detailed in Figure 5.

Hydrogen-Deuterium Exchange Profile of α -Neurexin1

Examination of the final map provides an extensive look at the structural nature of α neurexin1's LNS 4, 5 and 6. Initial fragmentation yielded the following sequence coverage for the whole protein: 93% for calcium deficient, 94% for calcium enriched, 83% for neuroligin-bound complex at 1:1.2 neurexin:neuroligin mole ratio, and 88% for neuroligin-bound complex at 1:3 neurexin:neuroligin mole ratio. Upon completion of the experiment, these shifted to 75%, 77%, 75%, and 70% respectively. Thus a majority of the LNS 4, 5, and 6 domains were recovered and deuteration data could be effectively quantified. LNS 4 coverage, with one disulfide bond, stayed around 83% for calcium deficient, calcium enriched, and 1:1.2 ratio and decreased slightly to 82% for the 1:3 ratio experiment. LNS 5, also with one disulfide bond, showed a similar trend where most experiments hovered at 77% coverage except for the 1:3 ratio experiment where it dropped to 58%. EGF 3 which is a small exposed domain held together by three disulfide bonds, yielded no data for the first three conditions, but provided a 39% coverage for the last. Finally LNS 6 gave 76% coverage for the first three conditions and yielded 73% for the 1:3 ratio. All of the following data are illustrated in Figure 6a-d. Peptide yields for each set came out to 303, 319, 233, and 150 peptides respectively. In this sequence there are 2 gaps at glycosylation sites found on Asn813 in LNS 4 and Asn1246 in LNS 6 which are characteristic of carbohydrate attachments which can significantly affect peptide affinity in solution, making it difficult to be properly ionized and analyzed by the mass spectrometer. Because Proteome Discoverer is not set up to identify peptides with complex carbohydrates attached, we are unable to recognize this

shift and account for it in its peptide identifications. In addition LNS 5 possesses gaps spanning Ala1040-Ile1051 which is between β sheets 10 and 11, leaving it as an unstructured region identified as its hypervariable region exposed to solution and digestion by protease, as well as Phe1094-Gly1105 which serves as an exposed linker to the EGF 3 domain. Even so, coverage of the three LNS domains studied was sufficient to show where specifically calcium and neuroligin associate.

In comparing the changes between calcium enriched and calcium deficient conditions, we saw decreased rates of exchange in LNS 4 along its α helix 1 region and β sheets 3,8, and 11-14 regions, in LNS 5 along its α 1 region and β 1-4, 6-9, and 12 regions, and in LNS 6 along its α 1 and β 2-7, 10-12 regions (Figure 6a-b). From prior literature we know that LNS 6's β 10 region flanks its hypervariable area where calcium can associate at concentrations as little as several hundred μ M and be fully saturated under physiological conditions (Sheckler et al., 2006; Tanaka et al., 2011). It can also be noted that binding of calcium induces a small change in the Asp1252-Val1256 area just upstream which is indicative of conformational change to allow for proper cation coordination. In addition LNS 4 and 5 have previously been hypothesized to possess calcium binding properties along respective hypervariable regions and auxiliary coordination regions given that sites for such in LNS 6 at Ile1268 and Asn1270 for the former as well as Asp1199 and Val1216 for the latter are highly conserved when compared against LNS 4 and 5's domain alignments (Rudenko et al 1999). They yielded evidence for a lower affinity binding possibly due to the differences in polarity and spatial orientation of each participant residue in LNS 4 and 5 in comparison to LNS 6. It should also be noted that there is an insert between Leu806 and Lys816 which when

present is likely interfering with normal calcium coordination contributions. With evidence for stabilization by calcium illustrated in Figure 7a, there is good support for calcium potentially having water-mediated interaction with LNS 4 & 5.

When bound to neuroligin in a 1:1.2 ratio, LNS 4 regions α helix 1 and β sheets 1-4, 8, 9, 11, 13, & 14, LNS 5 β 1, 4, & 7-9, and LNS 6 α 1 and β 2, 4, 6, 7, & 10 all showed marked decreases in rates of exchange. The most expected of these are near LNS 6's hypervariable region where neuroligin coordinates directly and indirectly with neurexin residues such as Arg1171 so as to potentially minimize steric and charge limitations caused by bulky side chains by sequestering it in a pocket formed by neuroligin's His267, Glu270, and Leu363 (Arac et al, 2007; Leone et al, 2010). While this may induce a conformational change characterized by increased flexibility across a segment of neuroligin, these residues ultimately contribute to the stability and functionality of the adhesion protein complex.

Upon analysis of the complex at the 1:3 bound ratio, one sees further slowing of LNS 4 α 1 and β 1-3 & 8-11, LNS 5 3-5 & 7-8, and LNS 6 α 1 and β 2-4, 6-7, & 10-13, a majority of which were seen to show notable when measured in stoichiometric ratios. Of these the greatest change was observed near the β 10 region of LNS 6, indicating that even with such an excess of neuroligin present, binding is still highly specific to the LNS 6 region along with any peripheral interactions which occur as a result of the LNS 6 anchor. Impact on deuteration is consistent with this mode of binding rather than separate neuroligin molecules binding at all three LNS domains. Thus it affirms that even when mole ratios are increased to such proportions, neuroligin continues to exhibit

high selectivity for LNS 6 binding and does not initiate binding to other α -neurexin LNS domains (Figure 7b-c).

Hydrogen-Deuterium Exchange Profile of β -Neurexin1

Analysis of the significantly shorter β -neurexin1 yielded coverage similar to that obtained with α -neurexin1 fragmentation. The initial digest yielded 97% coverage for the first three previously mentioned conditions. Upon completion of analysis final coverage came out to 93%, 95%, and 92% respectively. Peptide yields came out to be 215, 233, and 166 respectively. For a protein of such size with no disulfide bonds this information was enough to establish a suitable picture of interaction. Furthermore β -neurexin1 was expressed in bacteria which were not capable of providing the usual glycosylation at Asn184, a residue whose glycosylation does not affect expression.

When calcium is added there are shifts in exchange rates along the α 1 region as well as β sheets 1-4 & 6-13 with majority of change being around β sheet 10 (hypervariable region) just after splice site 4 which functions as the primary calcium binding site (Figure 8a-b, 9a). When the splice insert is present synaptic activity is pushed towards operating as in a GABAergic role (Craig and Kang, 2007). This sort of conformational shift was anticipated since side arms Asp137, Val154, Ile236, Asn238 directly interact with calcium to hold it tightly in place where it has been shown to assume an octahedral type geometry (Rudenko et al., 1999; Tanaka et al., 2011). As neuroligin was added, we noticed a change in the exchange rates such that the hypervariable region along with the residues interacting with calcium in β sheets 5 & 6 were being physically occluded by binding (Figure 8b-c, 9b). Furthermore Pro106 and

Ser107 in between β sheets 2 & 3, Leu135 between β 4 & 5, and Leu234 and Ser239 right before β 11 all contribute to Van der Waals interactions, Arg109 and Arg232 help form putative salt bridges, and Asn103, Arg105, Arg109, Tyr235, Asn238, and Ser239 form putative hydrogen bonds to neuroligin residues and stabilize the complex (Fabrichny et al, 2007). Outside of those regions, less significant changes were observed in portions of the remaining sequence. This likely indicates that binding to neuroligin once calcium is present does not necessitate large scale remodeling of β neurexin itself.

Hydrogen-Deuterium Exchange Profile of Neuroligin4

As a large dimeric molecule we expected neuroligin to be a challenge to resolve completely. Upon completing initial fragmentation optimization, we were presented with 93% coverage for calcium deficient condition, 95% for calcium enriched, 91% for 1:1.2 neuroligin: α -neurexin complex, and 91% for neuroligin: β -neurexin complex. Upon completion of analysis coverage came out to 73% for calcium deficient, and 82% for the final three conditions. Peptide yielded came out to 422, 422, 364, and 308 respectively. Two gaps seen in both sets are characteristic of glycosylations at Asn102 and Asn511. The structure also contains three disulfide bonds which are Cys110-Cys146, Cys306-Cys317, and Cys476-Cys510 which were all reduced when quenched. Final deuteration patterns also provide additional structural information for previously published crystal structures on His160-Ser164 and Pro539-Glu555 where their lack of structure prevented resolution by X-ray (Miller et al, 2011).

Review of deuteration experiments for calcium enriched neuroligin showed negligible to mild decreases in deuteration at α helices 4 (6,7) and 4 (7,8) and β sheets 6-

8 (data not shown). This transient increase in protection of these areas seems reasonable when comparative structures reveal that these are regions flanking or immediately linked to His267, Glu270, Gln359-Asn364, Asn462, and Tyr463 which are residues that interact with α and β neurexin. On the other hand we noticed some areas increase in flexibility or solvent exposure in response to calcium binding, particularly Val109-Leu114 which are at the N-terminus of the Cys loop, Asp158-Met169 which occupies the area immediately N-terminal to β sheet 3, as well as residues Tyr409-Leu416 which appear unstructured and feed into α 3 (7,8), the third α -helical region, along with Tyr549-Ala558 which has no organized structure.

Acquisition of data comparing binding to α neurexin and β neurexin yielded similar information. When bound to α -neurexin1, we observed a decreased exchange rate for the region between α 1 (6,7) and α 2 (6,7), α 2 (4,5), α 4 (6,7) and β 7, as well as α 4 (7,8) and β 8. There were also small increases in flexibility in the Cys loop α 1 (3,2) and α 3 (3,2) regions, α (3,4), 2 (7,8), α 2 (8,9) and β sheets 9-10 which likely coincided with a necessary rearrangement of the superstructure to facilitate binding (Figure 11a).

When bound to β -neurexin1, decreased rates of exchange are still observed between α 4 (6,7) and β 7, as well as α 4 (7,8) and β 8. What is interesting is that residues Asp385-Gly389 of Loop 2 also show signs of decreased exchange whereas α helix 1 (6,7) no longer exhibits difference in exchange when bound to β -neurexin1, indicative of a possible point of interaction that only α -neurexin1 is capable due to its other LNS domains (Figure 11b). In fact when bound to β -neurexin there seems to be a greater degree of exchange in that region along with regions of the unstructured N-terminus Leu58-Asp65, α (3,4), α 2 (7,8), α 3 (7,8), α 1 (8,9), and loop 3 (Figure 11c). The

differences here might be explained by the different regions of stabilization for neuroligin when bound to α -neurexin than when bound to β -neurexin and may play a role in how these two combinations might contribute to synaptic function differently.

Application of Deuteration Profiles to Crystal Structures

As mentioned previously an objective of these studies was to observe how the binding profile of neuroligin1 might differ between α - and β -neurexin. To do so, ribbon diagrams which utilize color codes to illustrate changes in deuteration profiles were applied to the crystal structure of neuroligin4- β -neurexin1 complex along with α -neurexin with its LNS 6 region superimposed on the neuroligin interface occupied by β -neurexin (data not shown), (Comoletti et al., 2007). Unfortunately we were unable to fill in a gap in the structure between Ile808-Lys816 due to a glycosylation at Asn813. Given the issue with retrieving glycosylated entities and the surrounding structure could not be resolved on its own, we conclude that it is likely a highly flexible region.

The rate of deuteration of a given protein is highly dependent on localized structuring. Areas which are not structured and/or are exposed to solvent deuterate the fastest. The hypervariable region of LNS 6 contains one such exposed area, is not spatially impeded by either of the other LNS domains, and exchanges with surrounding solvent so quickly it has become heavily labeled by quenching at 10 s, and fully labeled by 10,000 s as detailed by the yellow to red coloration at their corresponding locations in Figures 6a-b, 8a-b. The linker region between LNS 4's β sheet 14 and LNS 5's β sheet 1 is another example of such. On the other hand regions such as neuroligin4's α 2 (4,5) and α 4 (7,8) helices are buried within the structure and difficult for solvent to access even

after incubation for 100,000 s. From general review of the resulting structures we saw that the deuteration profiles of the respective proteins correlated with the respective crystal structures. Upon closer analysis of superimposed bound structures, we observe that α -neurexin1 LNS 6 domain's deuteration levels closely parallels that of β -neurexin1's. Thus we can reasonably conclude that having additional LNS domains attached does not alter how the LNS 6 domain interacts with neuroligin4, in addition to previous findings that additional LNS domains do not appreciably influence α and β neurexin binding affinity for neuroligin. (Miller et al, 2011)

Acknowledgement

The Results section, in part is currently being prepared for submission for publication of the material with the thesis author and coauthors Sheng Li and Palmer Taylor.

DISCUSSION

The purpose of this study was to identify any variations in the binding patterns of α -neurexin1's LNS 6 domain and β -neurexin1 under physiological conditions. In addition, we also wanted to examine whether neuroligin binding was specific to LNS 6/ β -neurexin or if it was capable of binding to LNS 4 & 5 at higher stoichiometric concentrations. The results on the association of neuroligin to neurexin would serve as a significant advance towards fully understanding the mechanistic details behind the causes of ASD as well as why an independent β -neurexin protein might have evolved.

Calcium's role as an indispensable binding partner

Previous studies have concluded calcium is a necessary component of neuroligin-neurexin interaction. For α -neurexin1 it has been shown calcium may associate with LNS 6 and potentially LNS 4 and 5, along with it needing to be bound for any binding to occur between neuroligin and neurexin. (Fabrichny et al., 2007; Miller et al., 2011; Sheckler et al., 2006) However little information is available about how its association can transiently alter distant conformations in the protein. For α -neurexin1, we demonstrate calcium binding induces a stabilization correlated with reduced exchange across the three LNS domains used (Figure 7a). Such is likely due to a combination of direct calcium coordination via residues in theoretical binding pockets of LNS 4 and 5 which have been speculated to have a lower affinity for calcium, along with residues Asp1199, Val1216, Ile1298, and Asn1300 in LNS 6, as well as conformational shifts which occurred as a result of binding (Miller et al., 2011 Tanaka et al., 2011)

β -neurexin1 possesses deuteration profiles similar to those of α -neurexin's LNS 6 which is a reasonable consideration given that the structural features are identical. On the other hand neuroligin does not show the similar marked shifts in deuteration when calcium was applied. A possible explanation for such is that upon analysis of the complex, the neuroligin residues do not all directly associate with calcium as β -neurexin1 residues do in a stable complex but rather utilize interactions of side chains Gln359-Asn364 to conduct a combination of direct calcium contact, water-mediated calcium contact, and residue-to-residue interaction.

Protein-Protein Interactions

Prior binding studies have offered significant insights on structural dynamics. In studying α -neurexin1 in complex at the 1:1.2 ratio, we observed characteristic binding at the hypervariable region of the LNS 6 domain and decreased exchange is observed in regions containing residues which are physically occluded by the presence of neuroligin as well as a small area of increased exchange characteristic of a necessary rearrangement to fully accommodate neuroligin (Figure 7b). In addition the β 11-13 regions and α 1 region of LNS 4 and β 4, 7-8 regions of LNS 5 exhibit further decreases in exchange likely due to an association with neuroligin4 that has successfully been anchored by LNS 6. Based on the deuteration results as well as the flexibility and location of the hinge region connecting LNS 5 to the EGF 3 domain neuroligin associates with more of the LNS 4 surface area than with the LNS 5 area, and when compared to known crystal structure data, these points of reduced exchange are consistent with previously mapped out regions where neuroligin is thought to be affiliated with (Miller et al., 2011; Tanaka

et al., 2012). When complexes are formed at 1:3 ratio stoichiometries, LNS 4's β 3, 8, 10-12 and α 1 regions as well as LNS 5's β 3-4, 7-8 exhibit even further decreases in exchange, while LNS 6 displayed the greatest changes of all three domains (Figure 7c). What this indicates is that even incubation at such high concentrations does not induce unspecific interactions between neuroligin4 and α -neurexin's LNS 4 and 5 domains of neurexin. Hence both α -neurexin and β -neurexin association occurs solely in a 1:1 stoichiometric ratio with neuroligin. Furthermore based on the neuroligin positioning in α -neurexin1 complex, LNS 4's changes come from interaction with neuroligin while changes in LNS 5 are a combination of occlusion by LNS 4 being brought spatially closer to its surface as well as minor indirect interactions with neuroligin binding. The setup for this affiliation necessitates the hinge region as described previously to twist slightly so as to place the LNS 6 binding site across from the faces of LNS 4 and 5 which show decreased exchange when neuroligin is present (Miller et al, 2011). On neuroligin's structure the corresponding regions of decreased exchange are spatially close to each other, indicating that α -neurexin1 does not necessarily assume a conformation where it needs to reach extensively around neuroligin but rather looks as if it pinches two points approximately 90° apart which might allow for enough space to dock LNS 6 and for LNS 4 and 5 to get close enough to induce the observed changes. Such an association is not possible for β -neurexin for its binding to neuroligin is restricted solely to one site. Even so when the deuteration profile of LNS 6 is applied to the crystal structure and superimposed on the neuroligin4: β -neurexin1 structural profile, the two show similar deuteration trends. Thus in addition to knowing that having additional LNS domains present does not noticeably alter the binding of LNS 6 to neuroligin4, it is shown that

having these additional domains present does not noticeably influence the structure of LNS 6. Furthermore with no changes in binding pattern, the reasons for such may likely be found in reasons of metabolic efficiency, survival against foreign molecules such as α -latrotoxin due to reduced synaptic docking sites, or simply providing synapse malleability where a difference in particular protein levels can influence synaptic transmission (Davletov et al., 1995; Tanaka et al., 2012).

Protein Structures in Solution

The role deuterium hydrogen exchange mass spectrometry plays in studying protein dynamics cannot be understated. The technique has allowed the elucidation of regions in proteins which may lack structure or for an otherwise precariously structured protein to be resolved in its entirety and complements information provided by protein NMR (Englander et al., 2003; Sharma et al., 2009). In addition some proteins may shift from a less structured state to a more structured one or vice versa when in contact with a particular binding partner, both of which can be examined via changes in their respective deuteration profiles (Wales et al., 2006; Wintrode et al., 2003). Furthermore, binding may cause a cascade of changes marked by cycles of loss of structure to restructuring into another conformation, as exemplified in studies on bovine spongiform encephalopathy disease (Colby et al., 2011; Liberski, 2012; Prusiner et al, 1984). With these changes proteins can become more structurally stable and even protease-resistant at times, which can be exemplified via substantial decreases in rates of deuterium hydrogen exchange. In general experimentation via DXMS allows for proteins to interact continuously under physiological conditions which can provide in some instances information which cannot

be obtained by other experimental methods (Hamuro et al., 2003). Thus far there has yet to be an X-ray crystal structure submitted detailing the interaction between neuroligin4 and α -neurexin1, but through the use of DXMS we have established that the proposed calcium-binding sites of LNS 4 and 5 are in fact capable of binding calcium under physiological conditions and that while our methodologies preclude us from designating exactly which residues may be interacting, we concur that a degree of function conservation took place in nature's delegation of responsibilities in the transition from α - to β -neurexin and that having additional interactions with neuroligin through LNS 4 and 5 may satisfy requirements for α -neurexin1 to functionally mediate calcium-dependent exocytosis along with the potential of regulating other processes which we do not yet understand (Missler et al., 2003). Together these may help fill in a vital part of the picture detailing how a mismatch in the neuroligin:neurexin complex occurs and lay down the groundwork for future studies on the neurological effects of when these novel regions of interaction are disrupted.

Evolutionary Pressures on Structural Designs

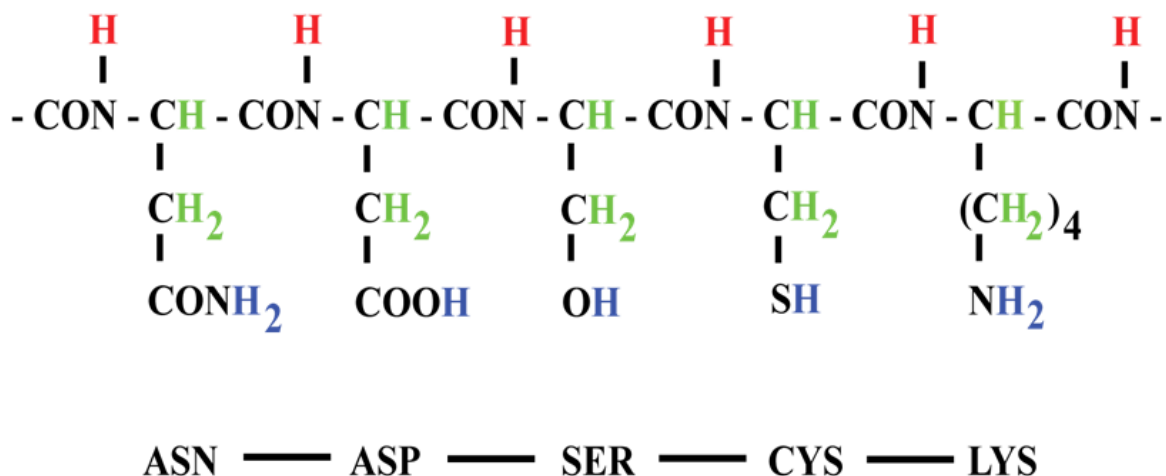
Evolution of survival niches and methods of coopting them have been in ceaseless competition for ages. Upon examining the data presented here and in previous studies one may ask why did a promoter region move downstream to solely include the last of six LNS regions of α -neurexin1 and thus creating an independent functional protein β -neurexin1. After all, this study established that LNS 6 is the primary binding site for neuroligin4 binding, and other studies have shown that β -neurexin1 can largely function in the same roles as α -neurexin1, likely saving the organism from seeming duplication.

However another plausible answer may be found in tolerating problems experienced in survival across the ages. For example in addition to its normal binding partners α -neurexin1 serves as a high affinity receptor for spider neurotoxin α -latrotoxin (Davletov et al., 1995; Sudhof, 2001). The toxin induces large-scale neurotransmitter release. Mechanistically it anchors onto the LNS 5 and 6 domains of α -neurexin1, likely through their calcium binding interfaces, and inserts itself into the presynaptic cell membrane, leading to neurotransmitter vesicle mobilization and exocytosis (Van Renterghem et al., 2000). It has been shown that such can occur both in calcium dependent and independent fashions. However the response is significantly stronger in the former and occurs through the use of α -neurexin's role as an integral regulator of neuronal calcium-dependent exocytosis. (Davletov et al., 1995; Hlubek et al., 2000; Missler et al. 2003; Ushkaryov et al. 1992; Ushkaryov et al., 2008; Volynsk et al, 2000; Zhang et al., 2005) On the other hand β -neurexin alone is unable to mediate the calcium-dependent exocytosis function that α -neurexin can and is seemingly unable to bind α -latrotoxin with sufficient affinity which likely prevents effectively insertion into the membrane and execution of its function. (Sudhof, 2001; Ushkaryov et al., 2008) Thus one might see the potential for the likely shift from a synapse containing solely α -neurexin on the presynaptic end to that of a mixture of α and β -neurexin so as to reduce the effectiveness of complications induced by molecules with functions similar to the toxin but still be able to preserve sufficient everyday function. However the precise reasons of this shift are still yet to be elucidated and should be further studied.

Acknowledgement

The Discussion section, in part is currently being prepared for submission for publication of the material with the thesis author and coauthors Sheng Li and Palmer Taylor.

FIGURES



H = Amide Hydrogen **H** = Carbon Hydrogen **H** = Side Chain Hydrogen

Figure 1: The three main groups of exchangeable hydrogen on amino acids are shown. Hydrocarbon-based hydrogens (green hydrogens) do not exhibit any measurable degree of exchange. Functional group hydrogens (blue hydrogens) exchange with solvent too rapidly for an accurate measurement to be made. Peptidic amide hydrogens (red hydrogens) exchange with sufficient rate and frequency to allow for accurate analysis by mass spectrometry and DXMS. (adapted from Hsu et al, 2009).

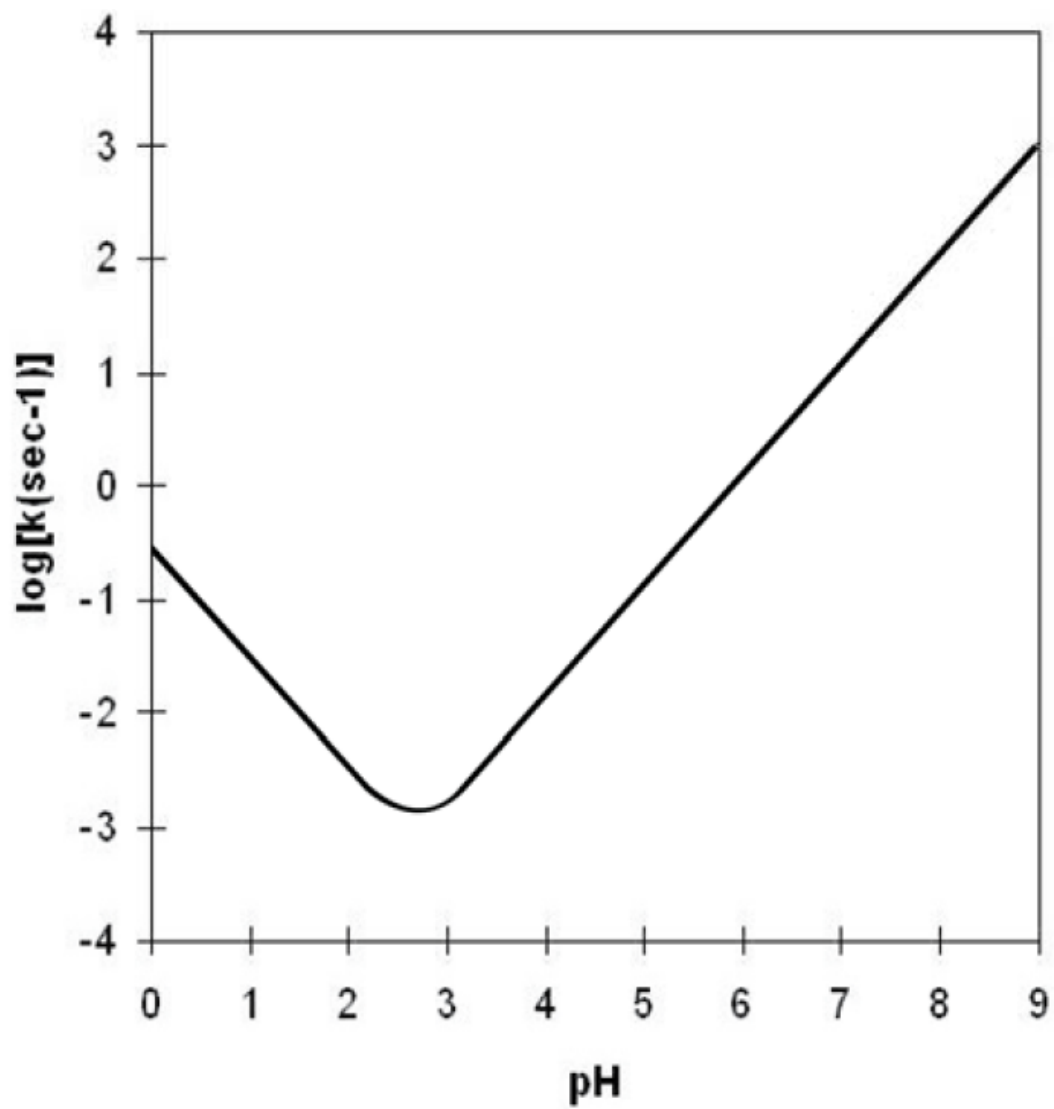


Figure 2: Rate of hydrogen/deuterium-exchange illustrated as a function of pH. Exchange rate is minimized at pH 2.5 (adapted from Tsutsui and Wintrode, 2007).

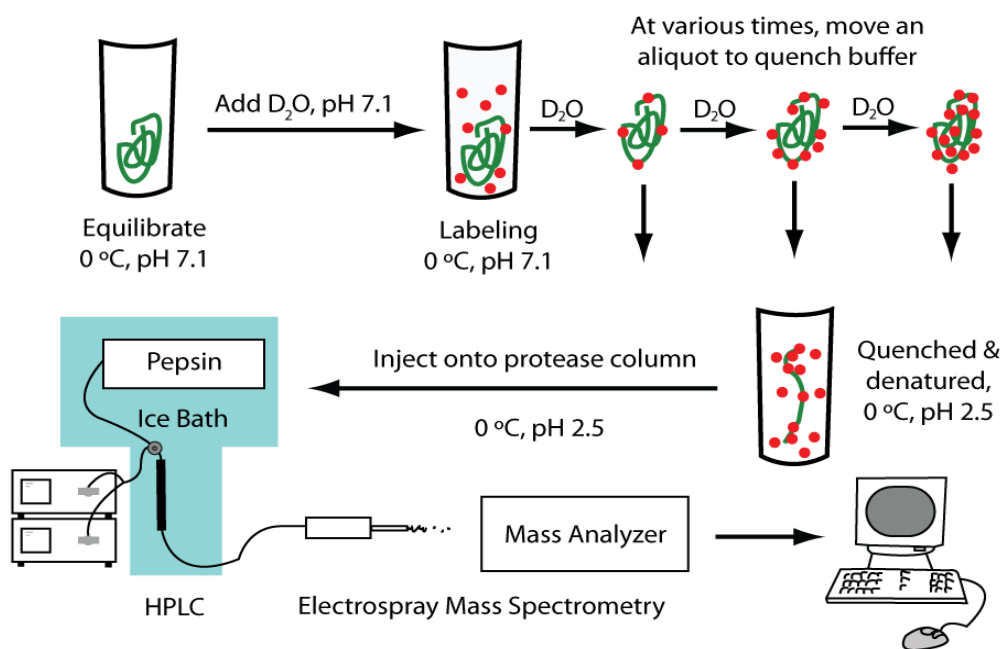


Figure 3: Schematic Overview of Deuterium Exchange Experiment Setup and Data Acquisition

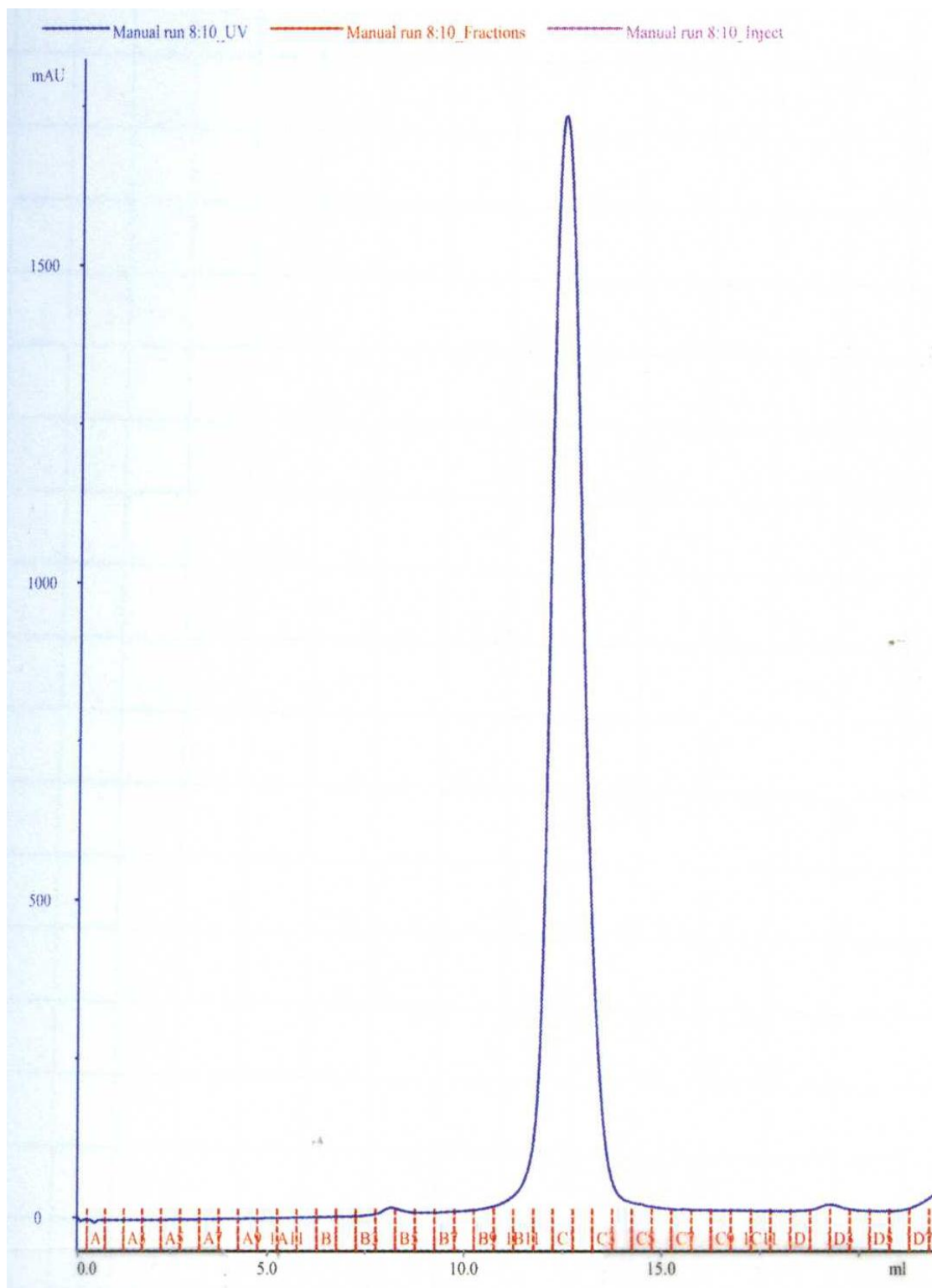
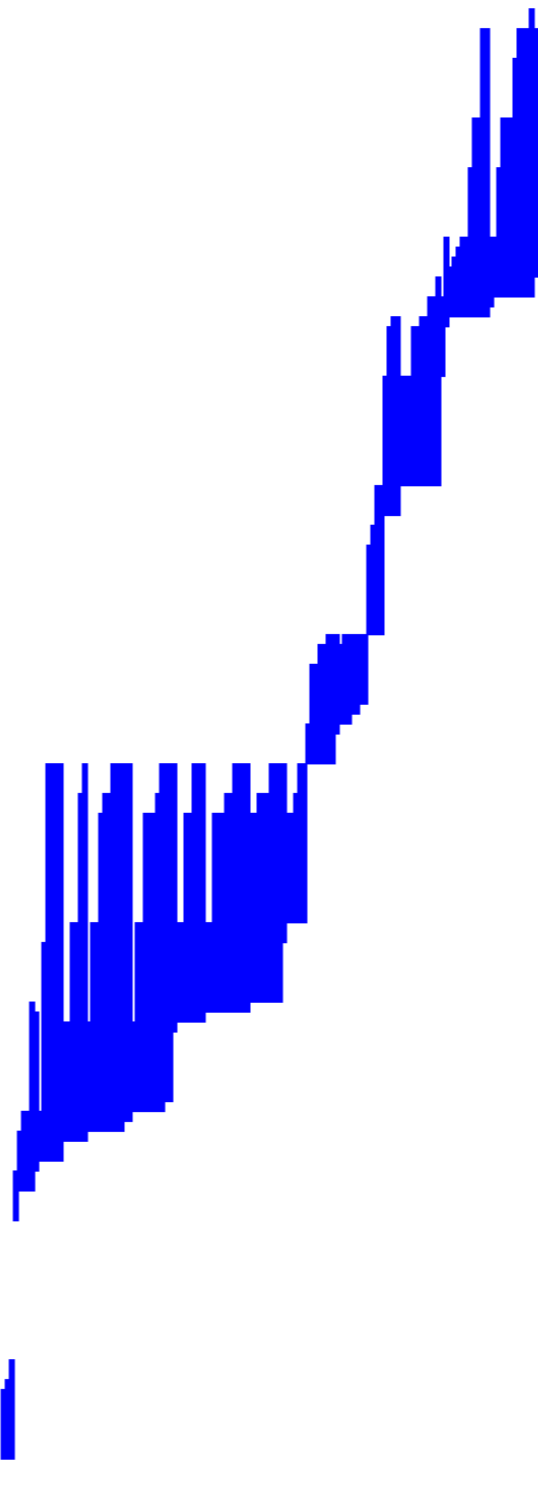


Figure 4: Chromatography analysis of Neuroigin4. Results show a well formed Gaussian peak with minimal extraneous material present.

Figure 5a: Fragmentation map for calcium deficient β -Neurexin1. Blue bars represent each individual peptide remaining after quality control analysis was performed and together they illustrate maximal potential coverage when performing deuterium exchange analysis. Subsequent figures follow suit. Similar maps were also plotted for α -Neurexin1 and Neuroligin4 which are not shown but detailed in Tables 1-3.

61
GPIGSPSSSLGAHHIHHFPGSSKHHSEVPIAIYRSPASLRGGHAGTTIFSKGGGOTYKWPNDORPSTRADRLAIGFTVQKEAVLYRVDSSSGLGVLELHHAGKI GVKFNVTGDDOIAIEESNAIINDGKYHVVRFRTRSGGNATLOV



81
NAILNDGKYHVVRFRTRSGGNATLOVDSWPVIERYPAGROLTIFNSQATIIIGGKEAGQPFAGQLSGLVYNGLKLINHAENDANIATVGNVRLVGEVPSSTTET

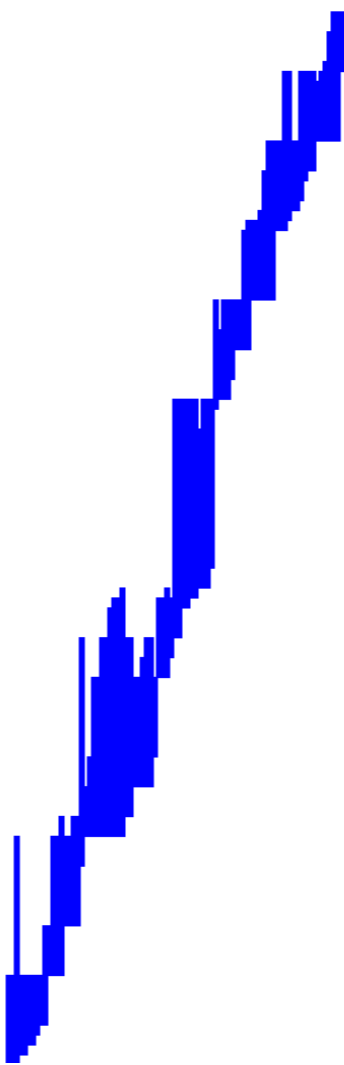


Figure 5b: Fragmentation map for calcium enriched β -Neurexin1.

41 GPLGGPNSSSLGARRHHNFAGSSKHHSTPIAIYRSPASLRGGHAGTTTIFSKGGGQITTKMPPNDPSTRADRLAIGFTVQKAPLVRYDSSSLGDTLLELHIHQGKI GVKFNVTODI ALEESNAI I NDGKYHVYRFTRSBGNATLOV

181

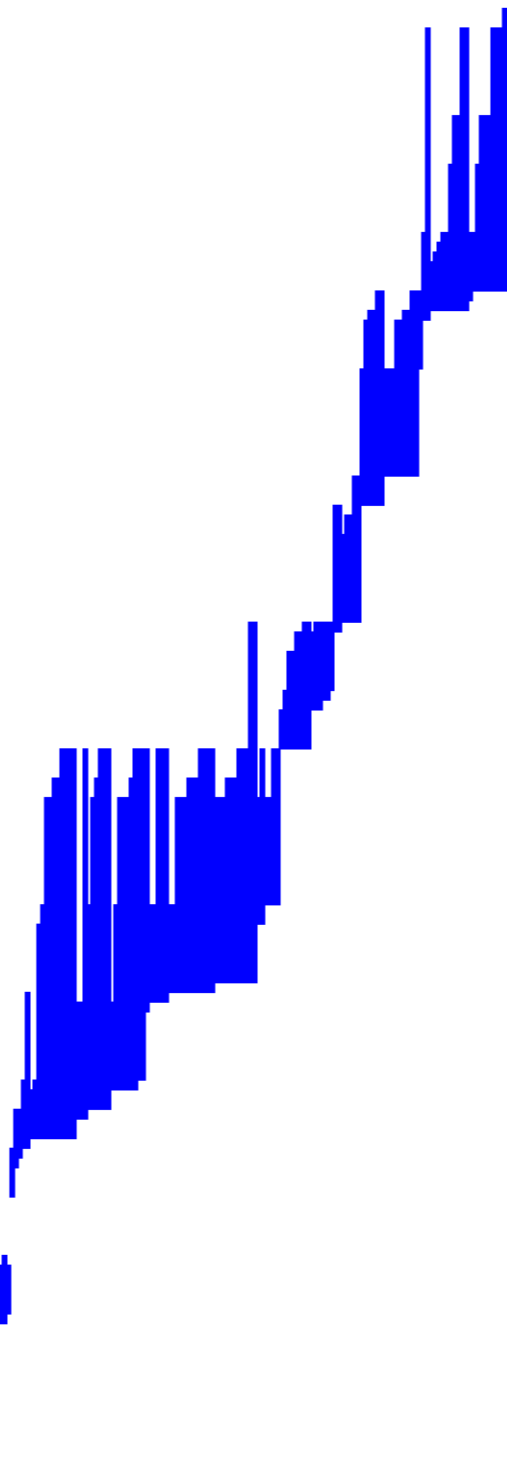
181

181

181

181

181



181 NAI I NDGKYHVYRFTRSBGNATLOVDSUPPIERYPAGROLTIFNSQATIIIGGKRGOPFRGOLSELYNGKLNMAKENDANIAYVGHURLIETPSSMTTEST

181

181

181

181

181

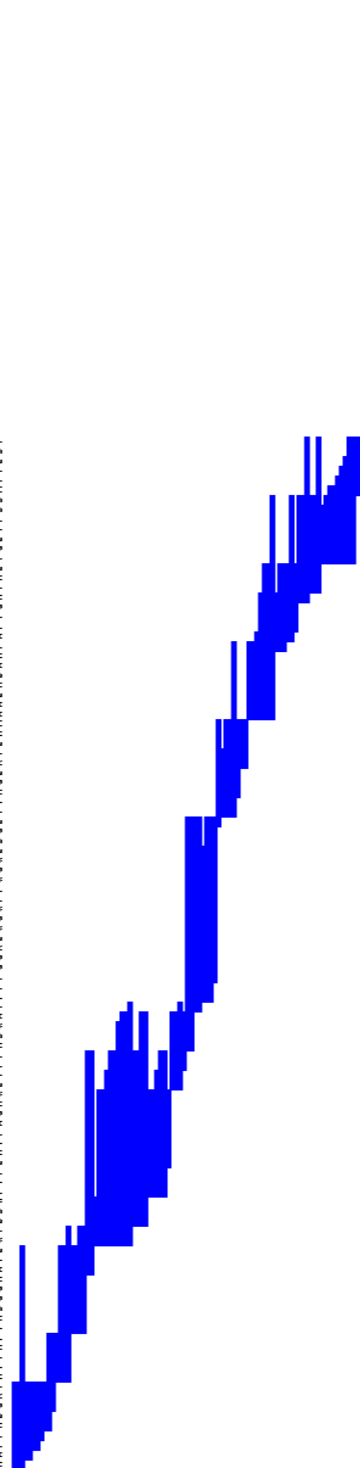
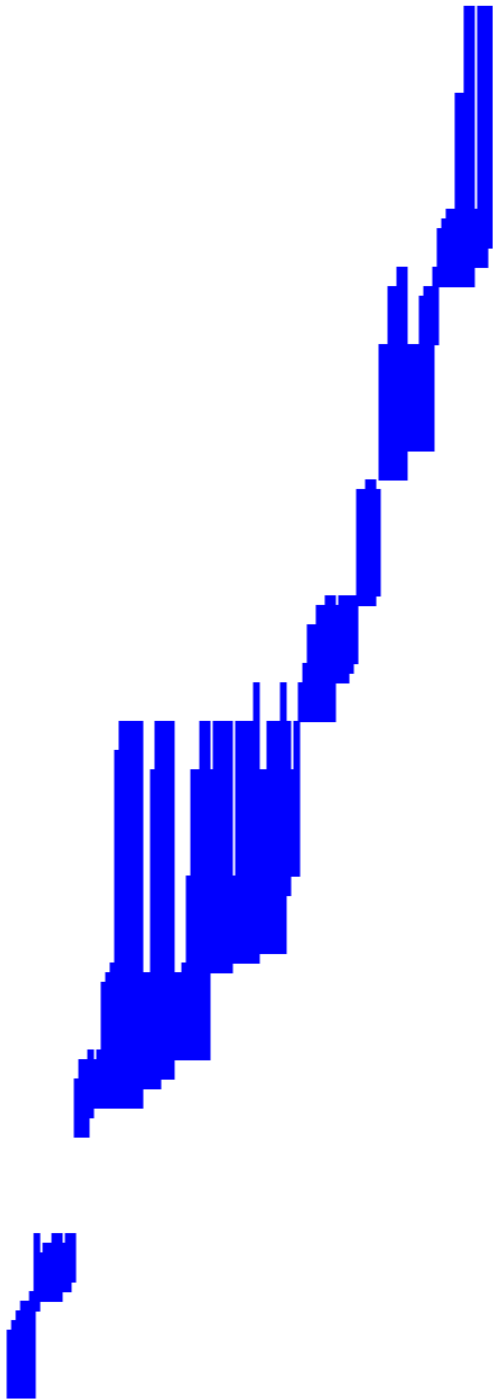


Figure 5c: Fragmentation map for β -Neurexin1:Neuroigin4 1:1.2 mole ratio complex.

41 GPLGSPNSSLGAAHHHAFAGSSKHHSTPIAIYRSPASLRGGHAGTTIFSKGGGLTYKWPFPNDPSTRADRLAIGFTYOKKATLVRVDSSEGLDYLELHHHGKI GYKFNVTDDI AIEESNAII IIOGKYHVVRFRSGGNATL



181 NAIIOGKYHVVRFRSGGNATLQDSWPVIERYPAGROLTI FNSGATIIIGGKGGOPFOGOLSGLYINGKVLNMAENDANI AIIIGNIRLVGEVPSMTEST

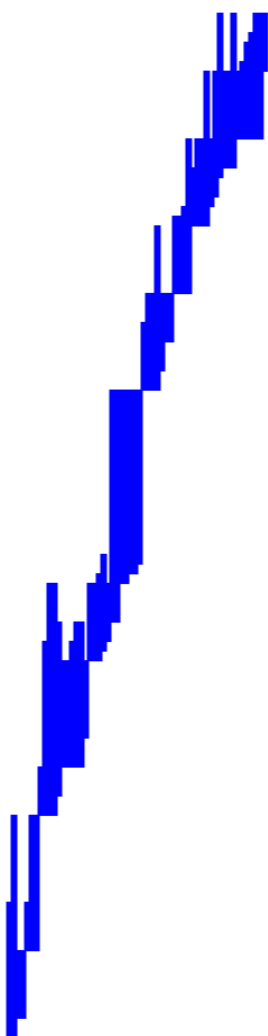


Figure 6a: Functional deuteration exchange profile for calcium deficient α -Neurexin1. The arrows denote the start of the LNS 4, LNS 5, EGF 3, and LNS 6 domains respectively along the amino acid sequence. Unstructured and unprotected regions tend to deuterate fastest and saturate early on, which is illustrated by the red coloring seen below respective portions of the sequence. More structured regions deuterate slower and overall levels can be observed via progression from blue band coloring to red band coloring. Finally occluded regions at the core incorporate deuterium slowly, if at all, and remain blue. Subsequent figures describe similar exchange behavior.

Ribbon Map of Alpha Neurexin alone (no Ca, D%, Deuteration Level)

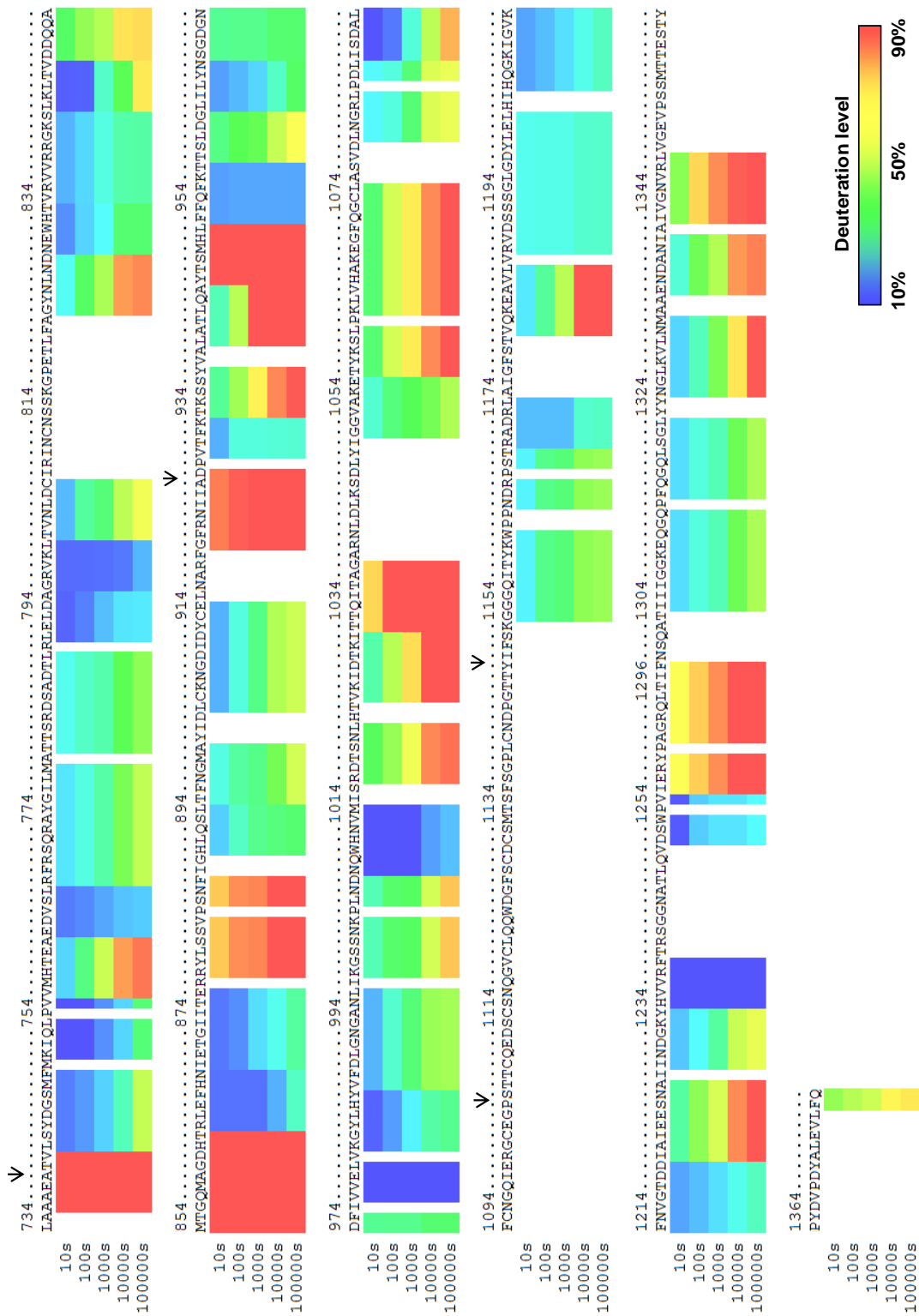


Figure 6b: Functional deuteration exchange profile for calcium enriched α -Neurexin1.

Ribbon Map of Alpha Neurexin alone (Ca, in D%, Deuteration Level)

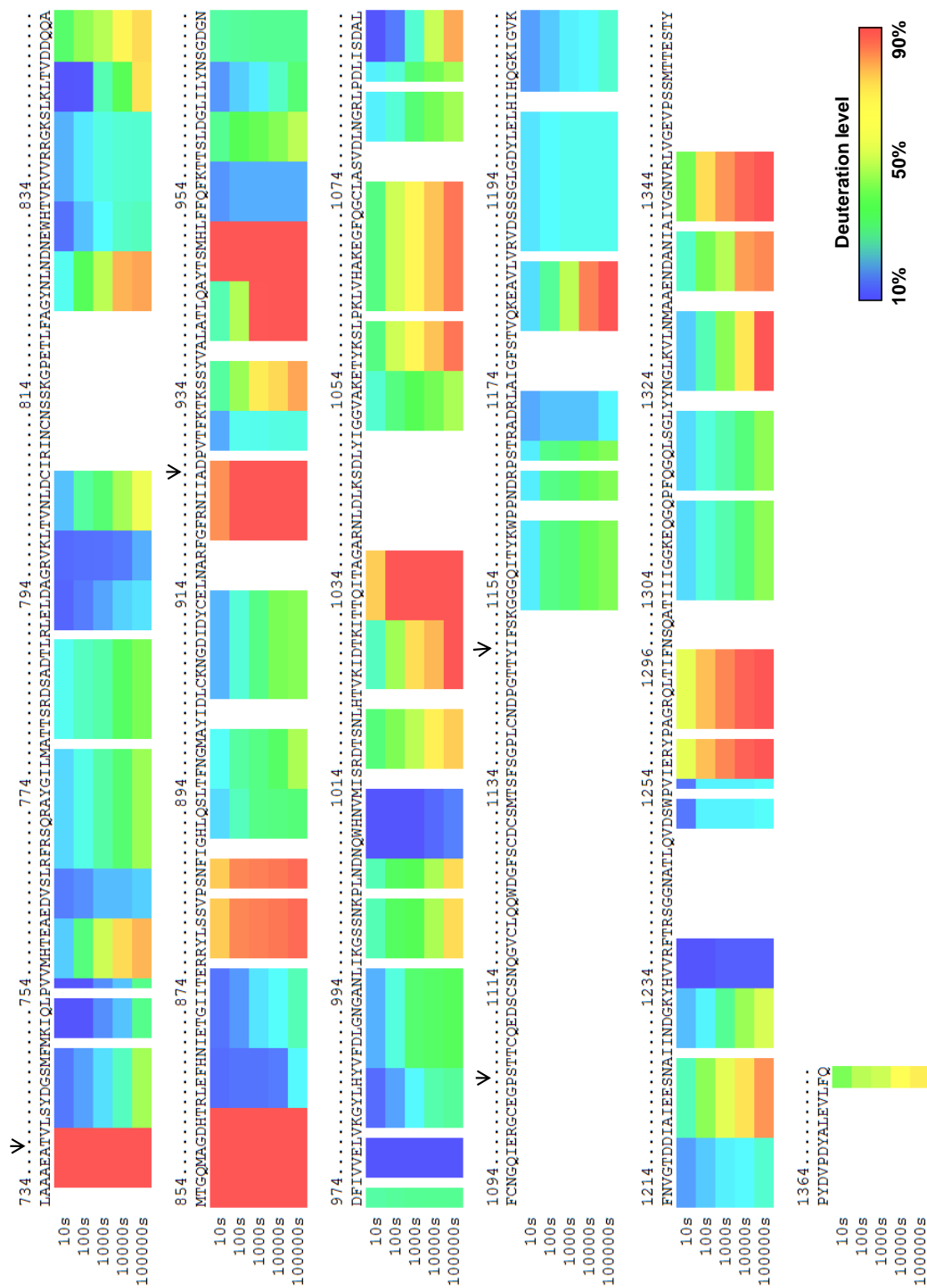


Figure 6c: Functional deuteration exchange profile for α -Neurexin1:Neuroigin4 complex at 1:1.2 mole ratio.

Ribbon Map of Alpha Neurexin in Complex (1:1.2, in D%, Deuteration Level)

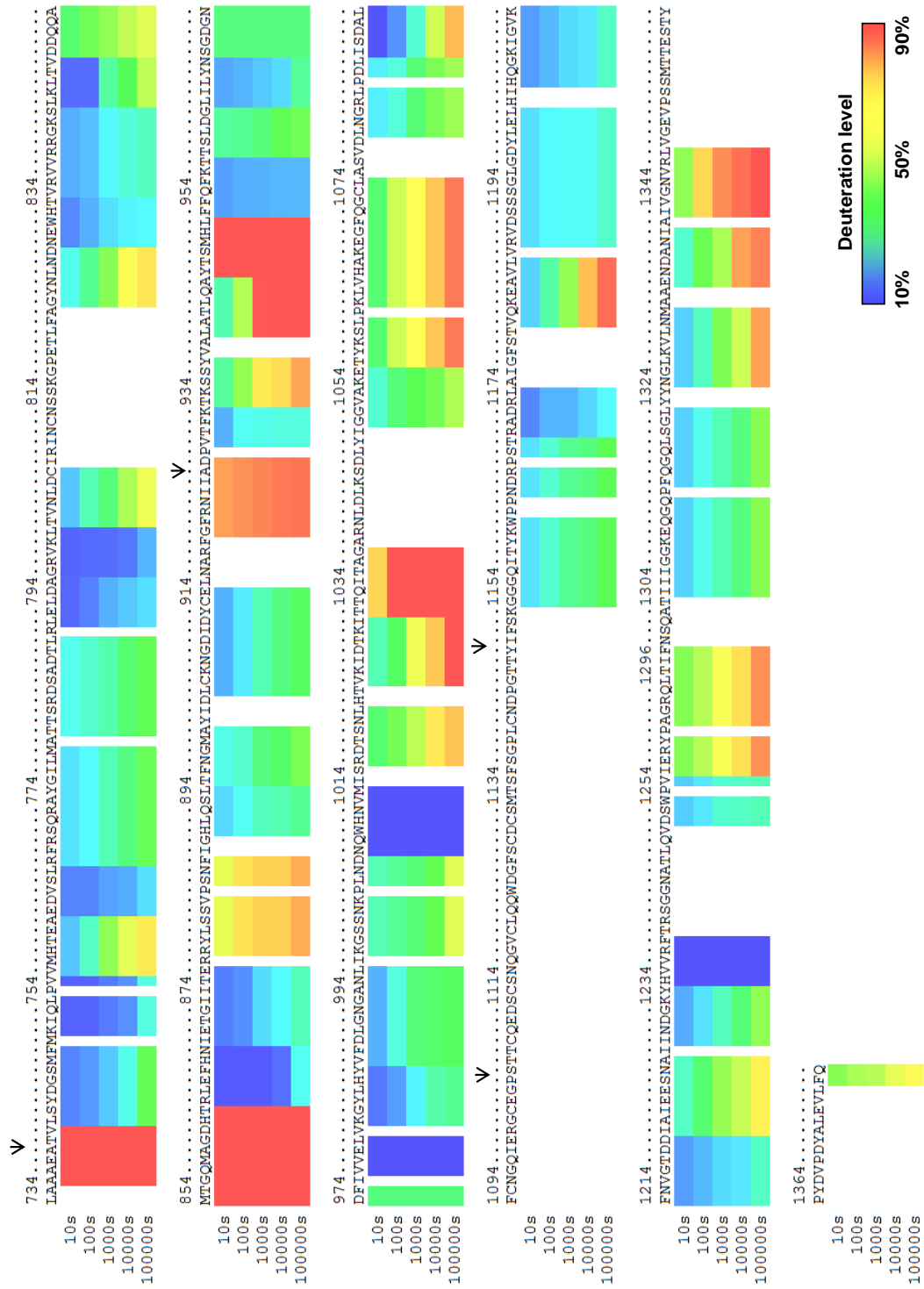


Figure 6d: Functional deuteration exchange profile for α -Neurexin1:Neuroigin4 complex at 1:3 mole ratio.

Ribbon Map of Alpha Neurexin in Complex (1:3, Ca, in D%, Deuteration Level)

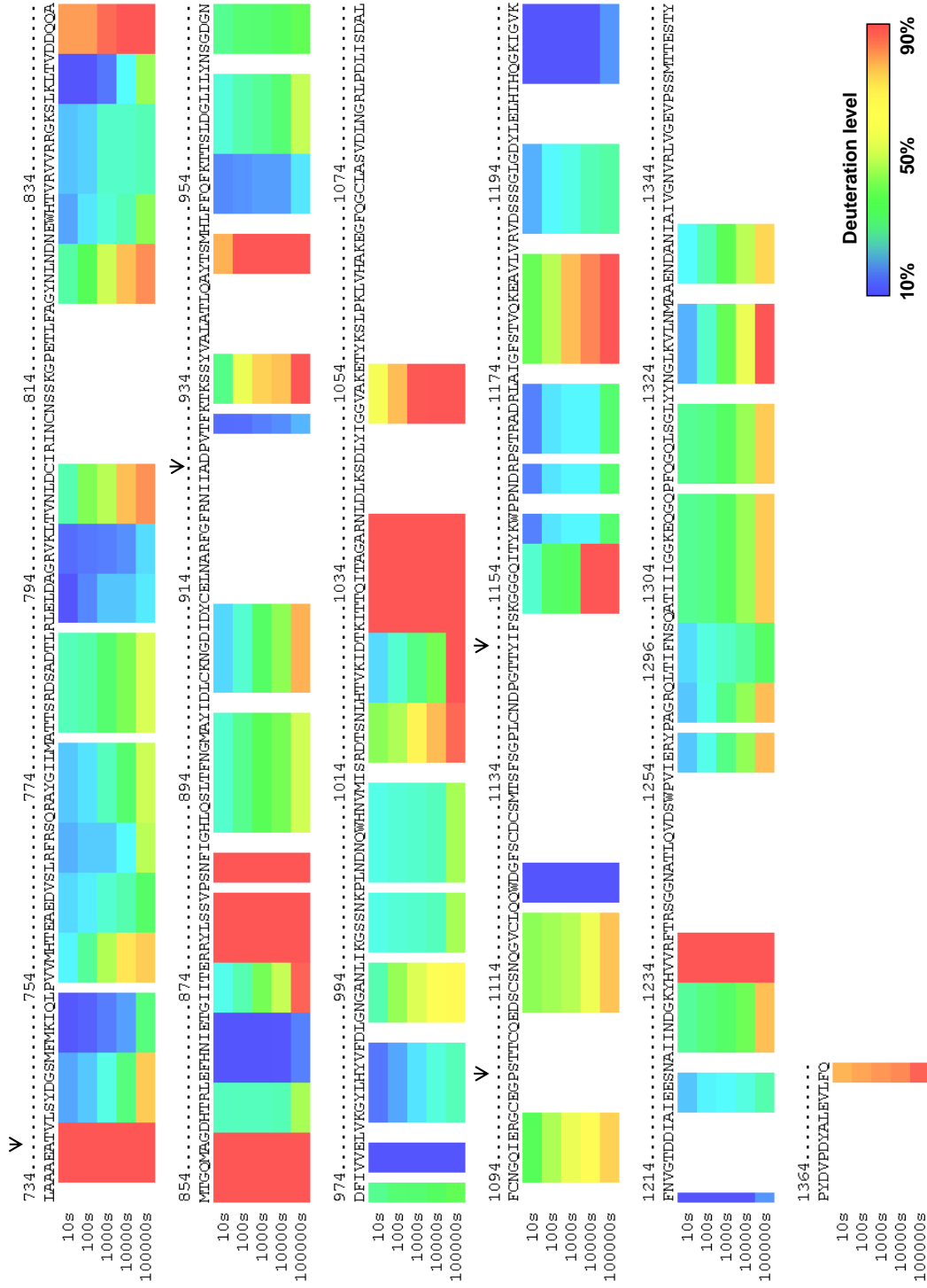


Figure 7a: Functional deuteration exchange difference map for α -Neurexin1 calcium deficient and calcium enriched conditions. Calcium deficient deuteration levels are subtracted from calcium enriched deuteration levels. Areas of blue illustrate graded increases in protection in the presence of calcium. Significance level was set to consider differences greater than 10%. Subsequent figures follow suit.

Alpha Neurexin in Complex (1:1.2) MINUS Alpha Neurexin Alone (Ca) (in D%, Deuteration Level)

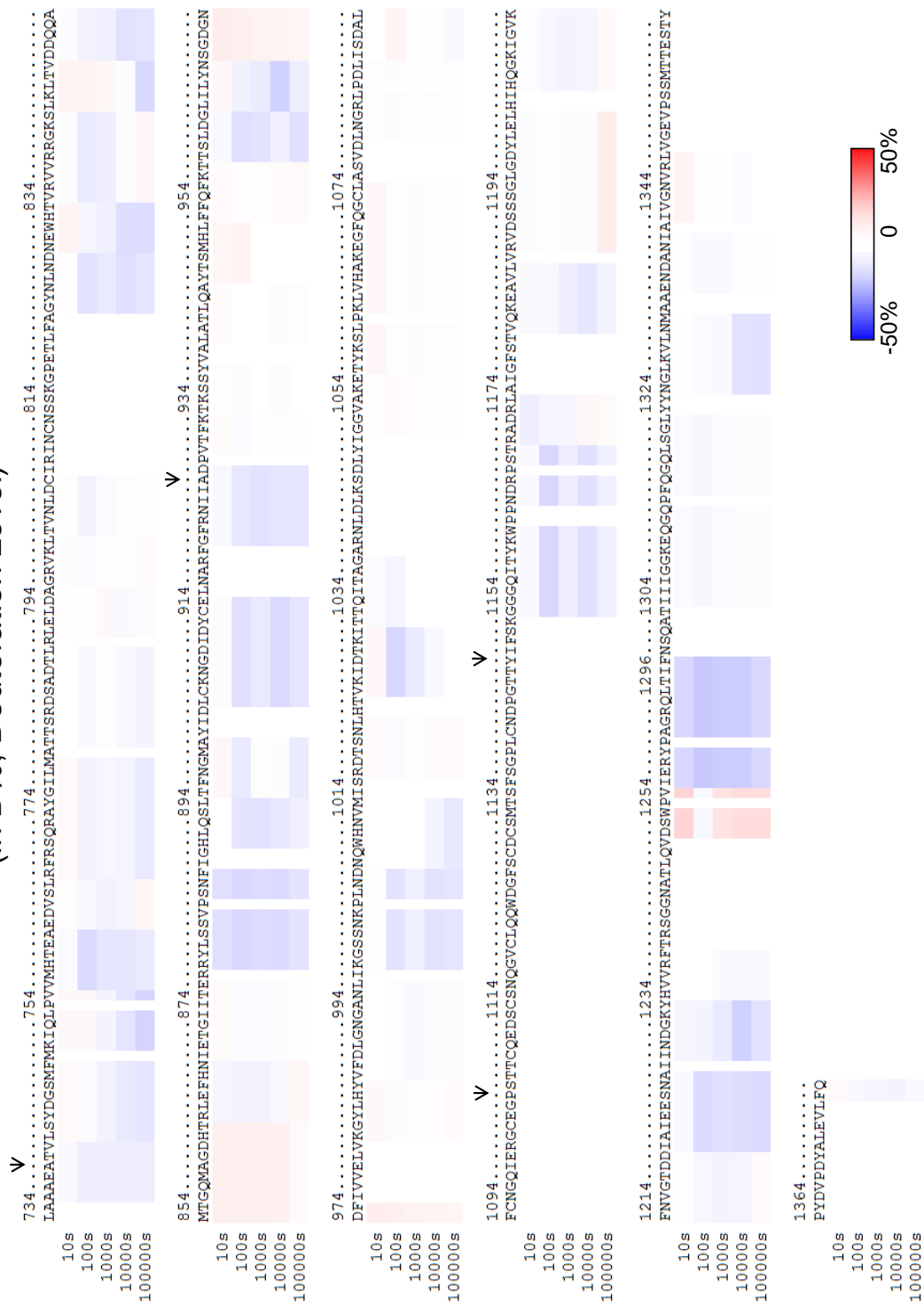


Figure 7b: Functional deuteration exchange difference map for α -Neurexin1 calcium enriched and α -Neurexin1:Neureoligin4 1:1.2 mole ratio complex conditions. Calcium enriched deuteration levels are subtracted from 1:1.2 deuteration levels.

Alpha Neurexin in Complex (1:1.2) MINUS Alpha Neurexin Alone (Ca) (in D%, Deuteration Level)

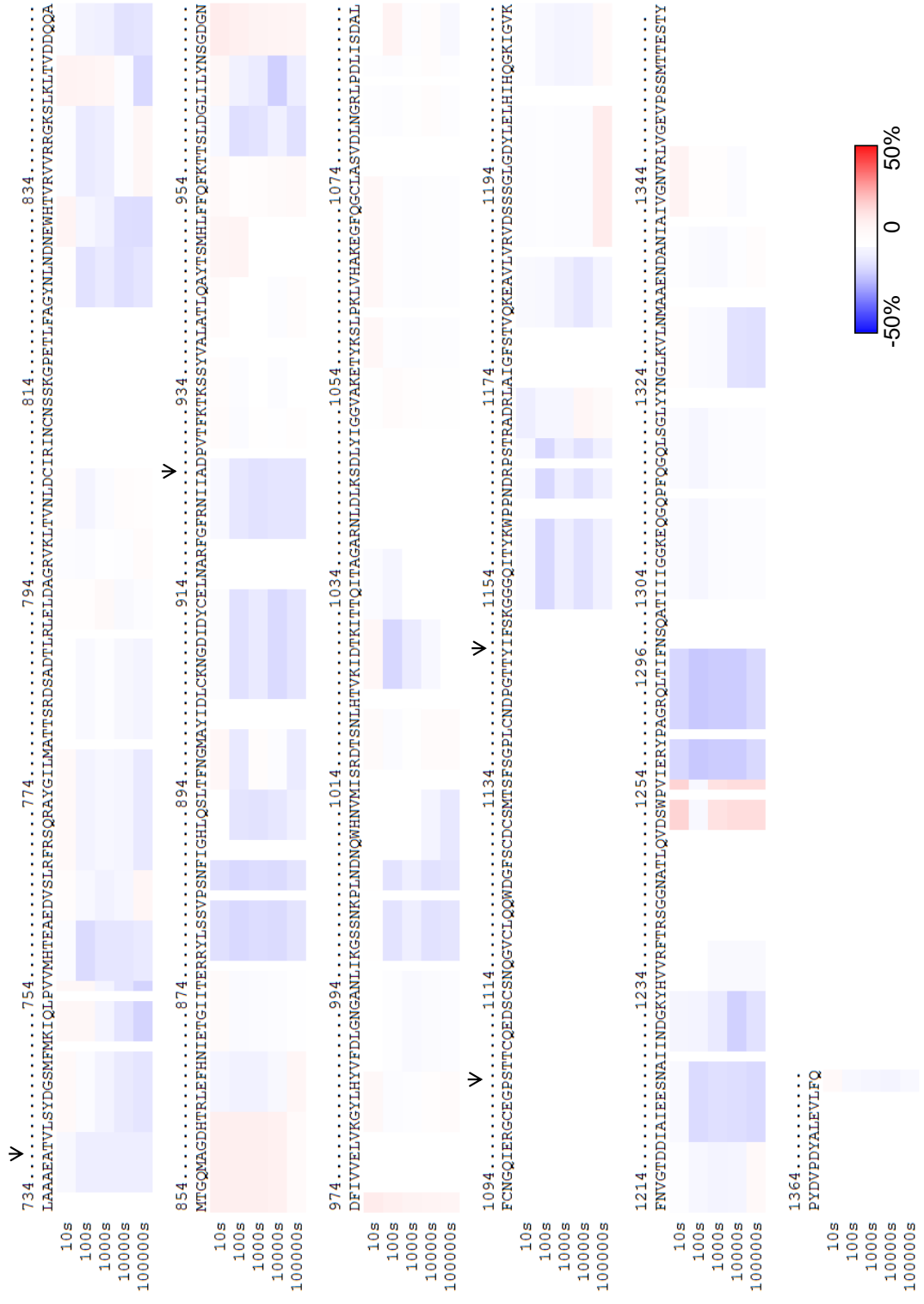


Figure 7c: Functional deuteration exchange difference map for α -Neurexin1 1:1.2 mole ratio complex and 1:3 mole ratio conditions. 1:1.2 mole ratio deuteration levels are subtracted from 1:3 deuteration levels.

Alpha Neurexin in Complex (1:3) MINUS Alpha Neurexin in Complex (1:1.2) (in D%, Deuteration Level)

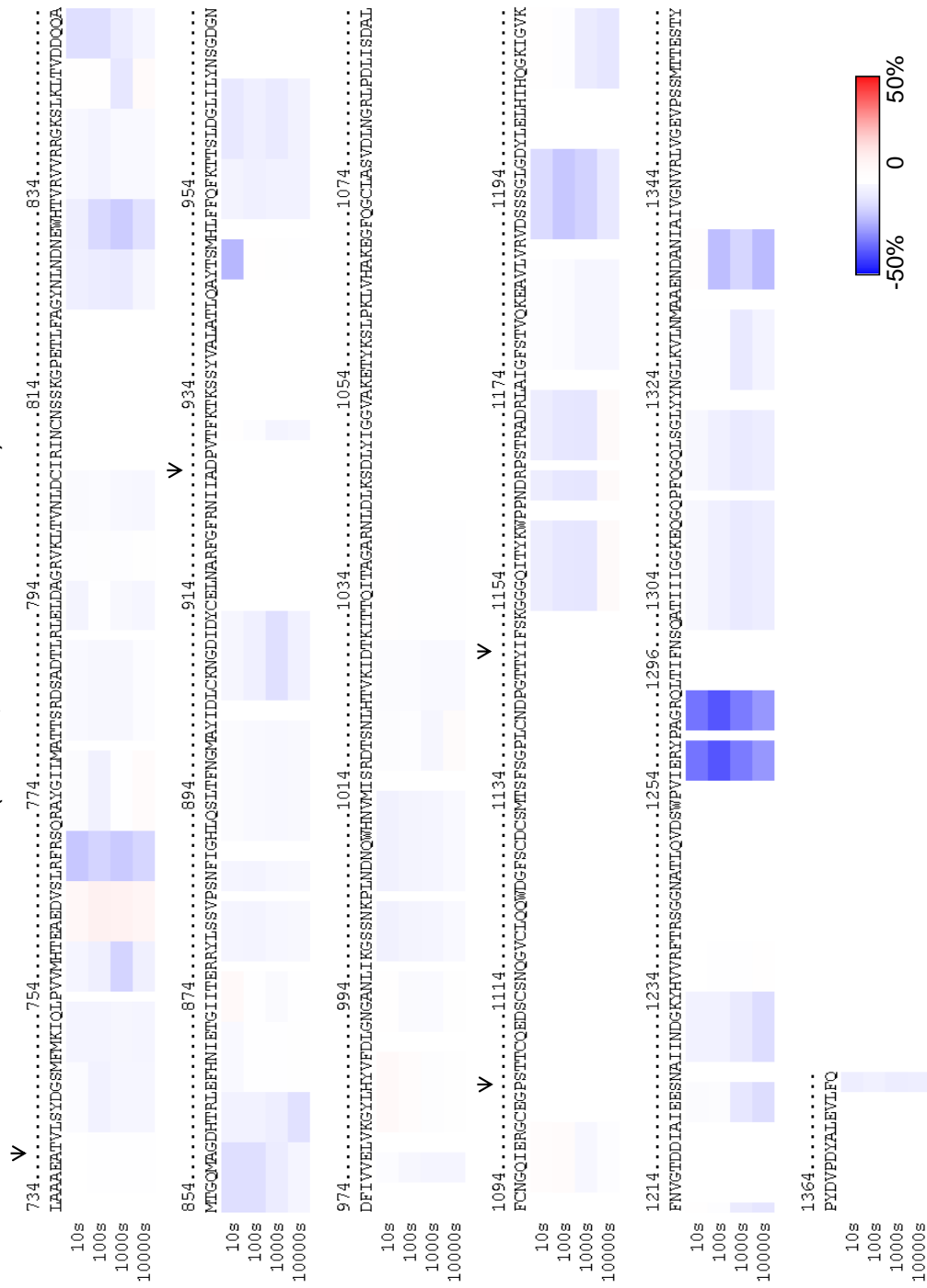


Figure 8a: Functional deuteration exchange profile for calcium deficient β -Neurexin1. As with figure 4, deuteration profiles are displayed under the amino acid sequence. The arrow denotes the start of the β -neurexin sequence. Subsequent figures follow suit.

Ribbon Map of Beta Neurexin alone (no Ca, in D%, Deuteration Level)

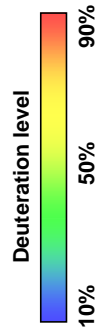
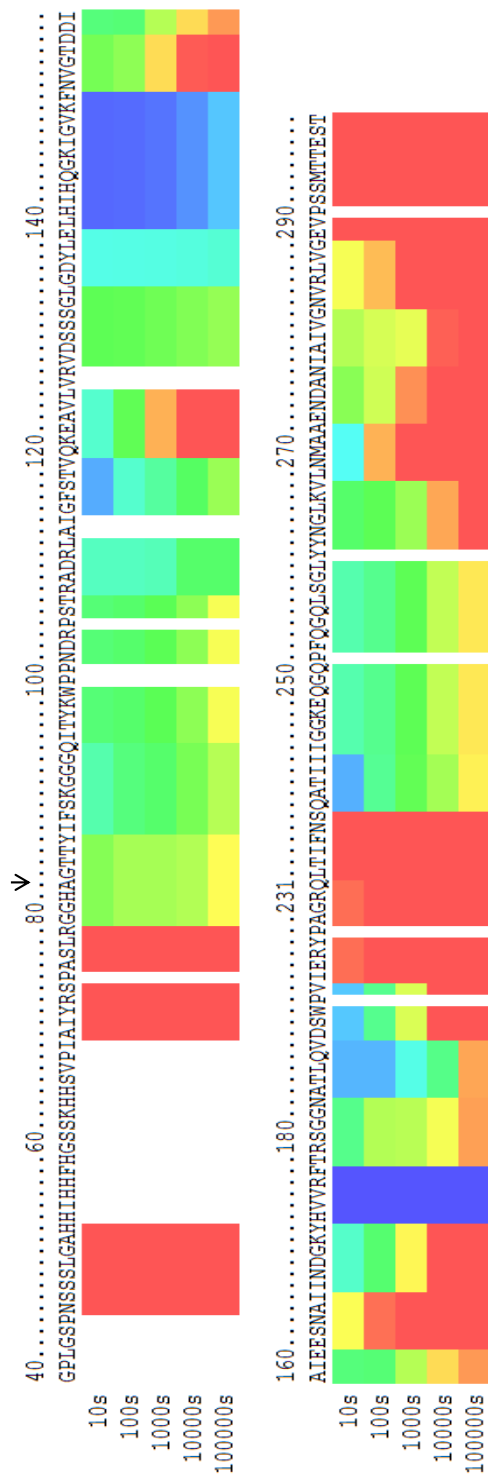


Figure 8b: Functional deuteration exchange profile for calcium enriched β -Neurexin1.

Ribbon Map of Beta Neurexin alone (Ca, in D%, Deuteration Level)

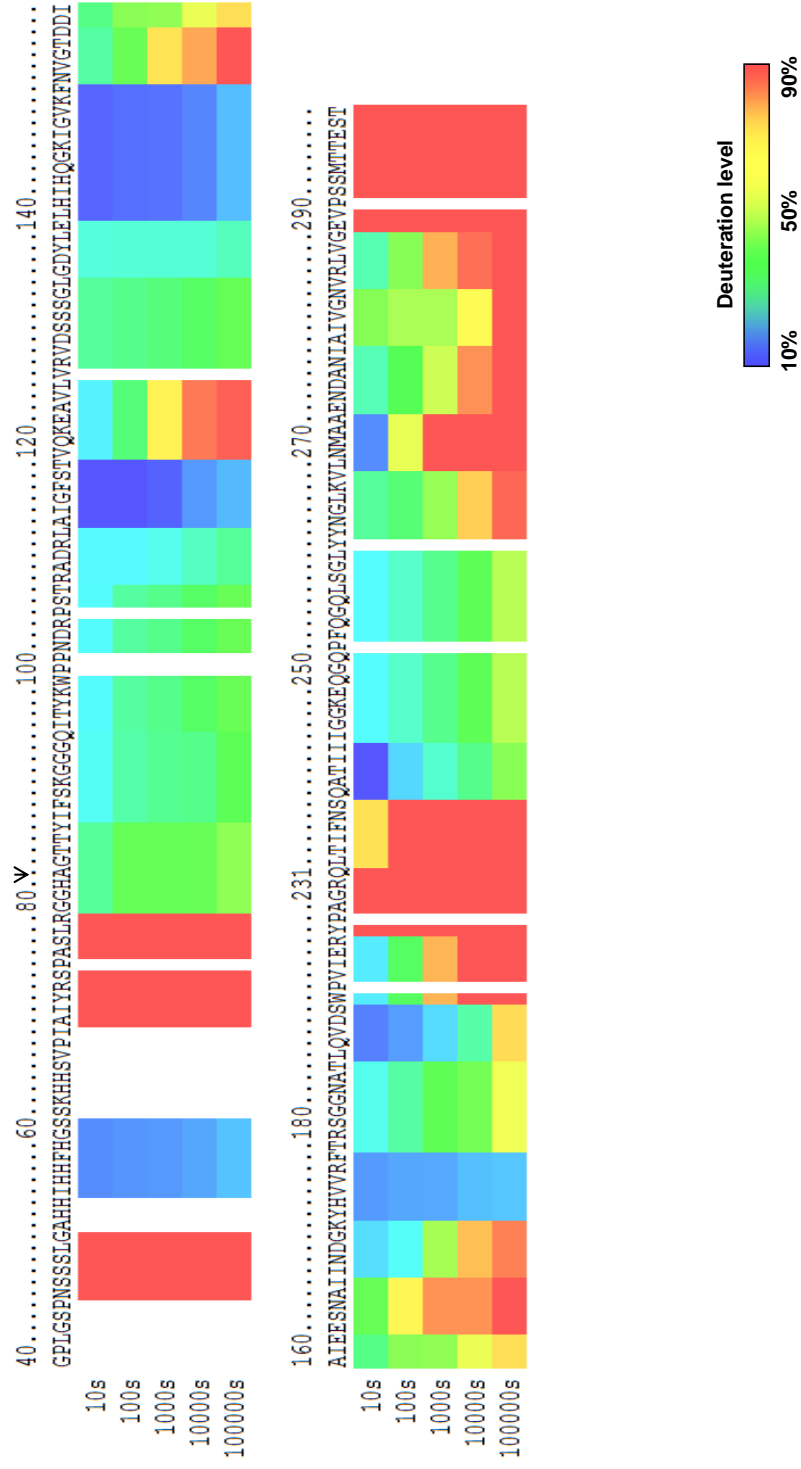


Figure 8c: Functional deuteration exchange profile for β -Neurexin1:Neuroigin4 complex at 1:1.2 mole ratio.

Ribbon Map of Beta Neurexin in Complex (1:1.2, in D%, Deuteration Level)

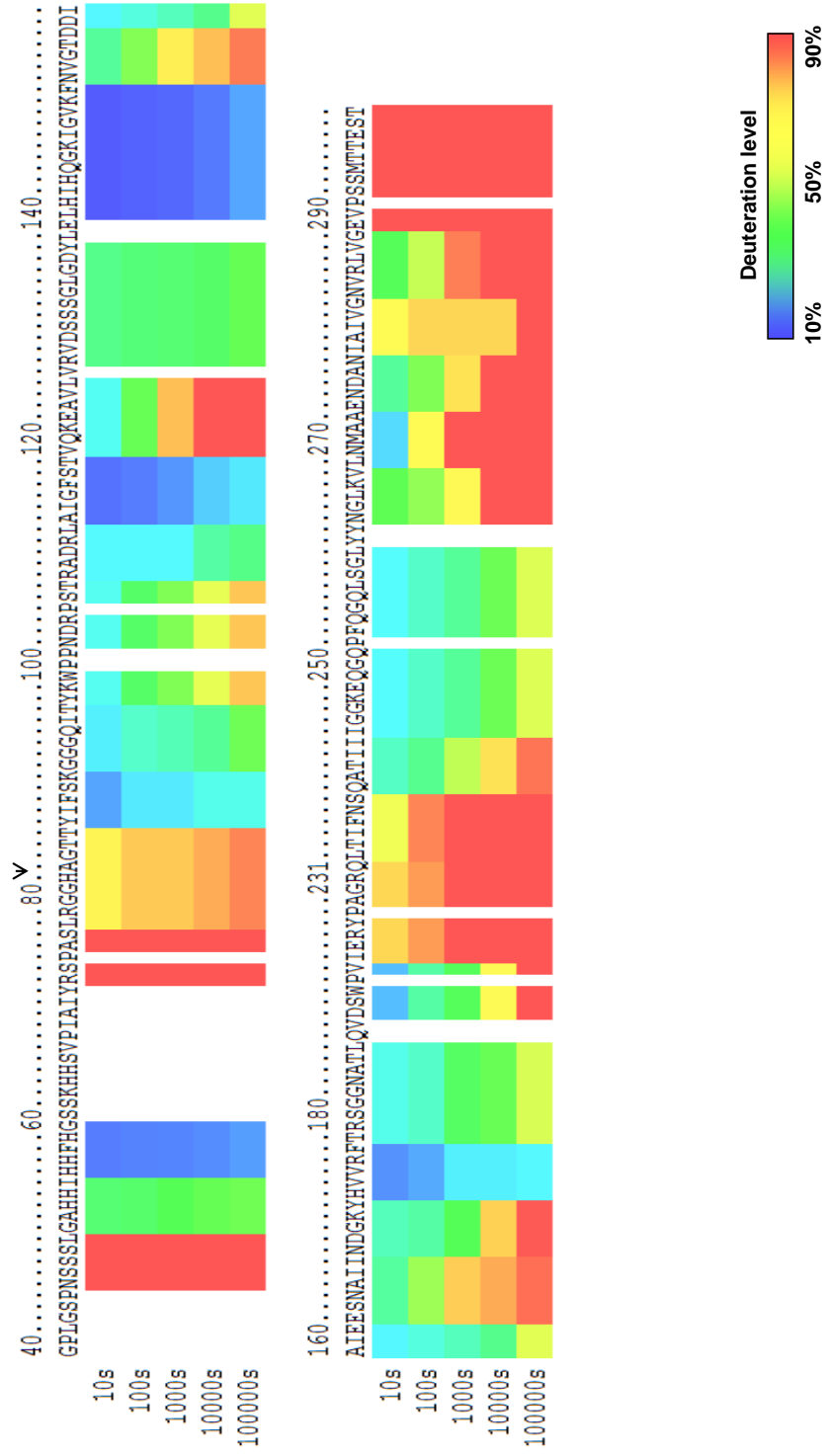


Figure 9a: Functional deuteration exchange difference map for β -Neurexin1 calcium deficient and calcium enriched conditions. Calcium deficient deuteration levels are subtracted from calcium enriched deuteration levels. Areas of blue illustrate graded increases in protection upon addition of calcium. Significance level was set to consider differences greater than 10%. Subsequent figures follow suit.

Beta Neurexin Alone (Ca) MINUS Beta Neurexin Alone (no Ca) (in D%, Deuteration Level)

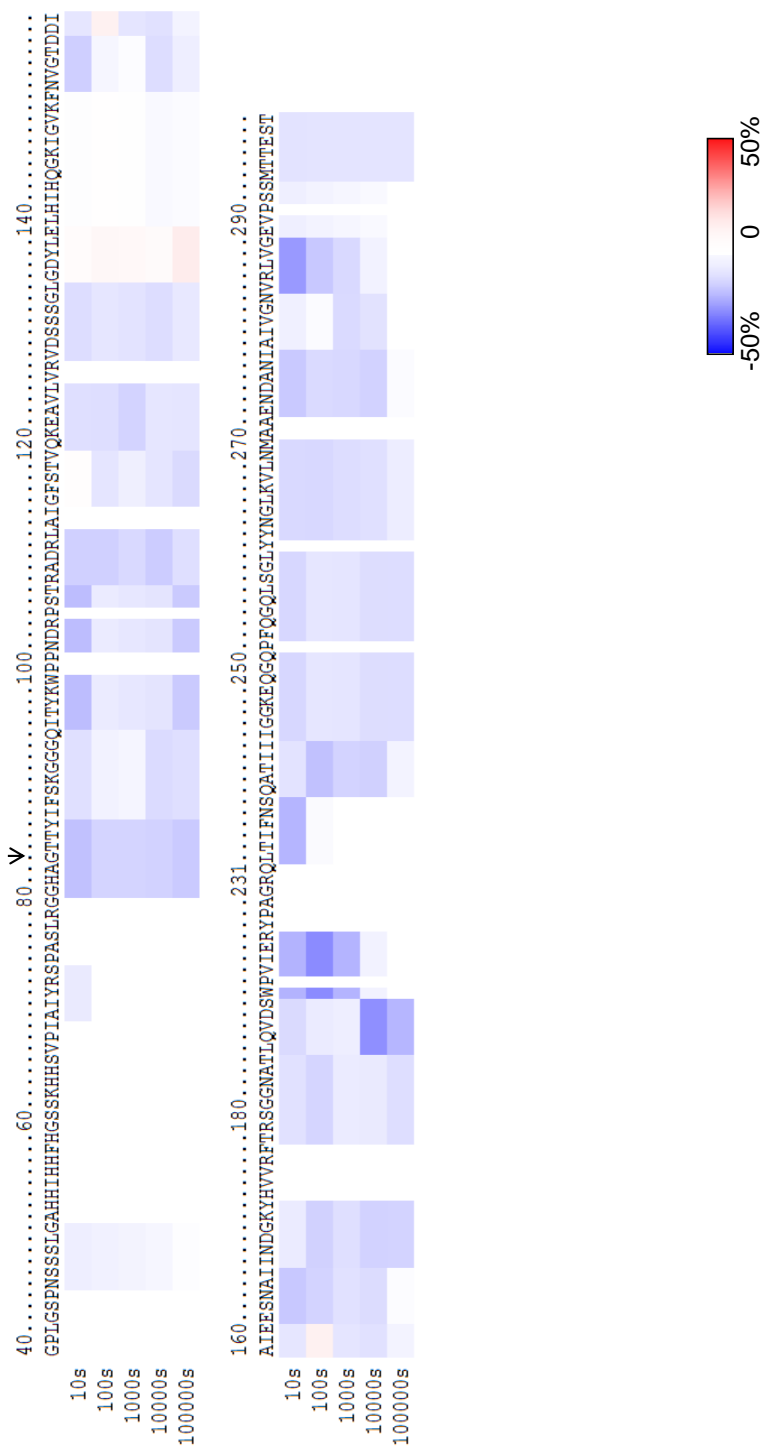


Figure 9b: Functional deuteration exchange difference map for β -Neurexin1 calcium enriched and B-Neurexin:Neuroigin4 1:1.2 mole ratio complex conditions. Calcium enriched deuteration levels are subtracted from 1:1.2 deuteration levels.

Beta Neurexin in Complex (1:1.2) MINUS Beta Neurexin Alone (Ca) (in D%, Deuteration Level)

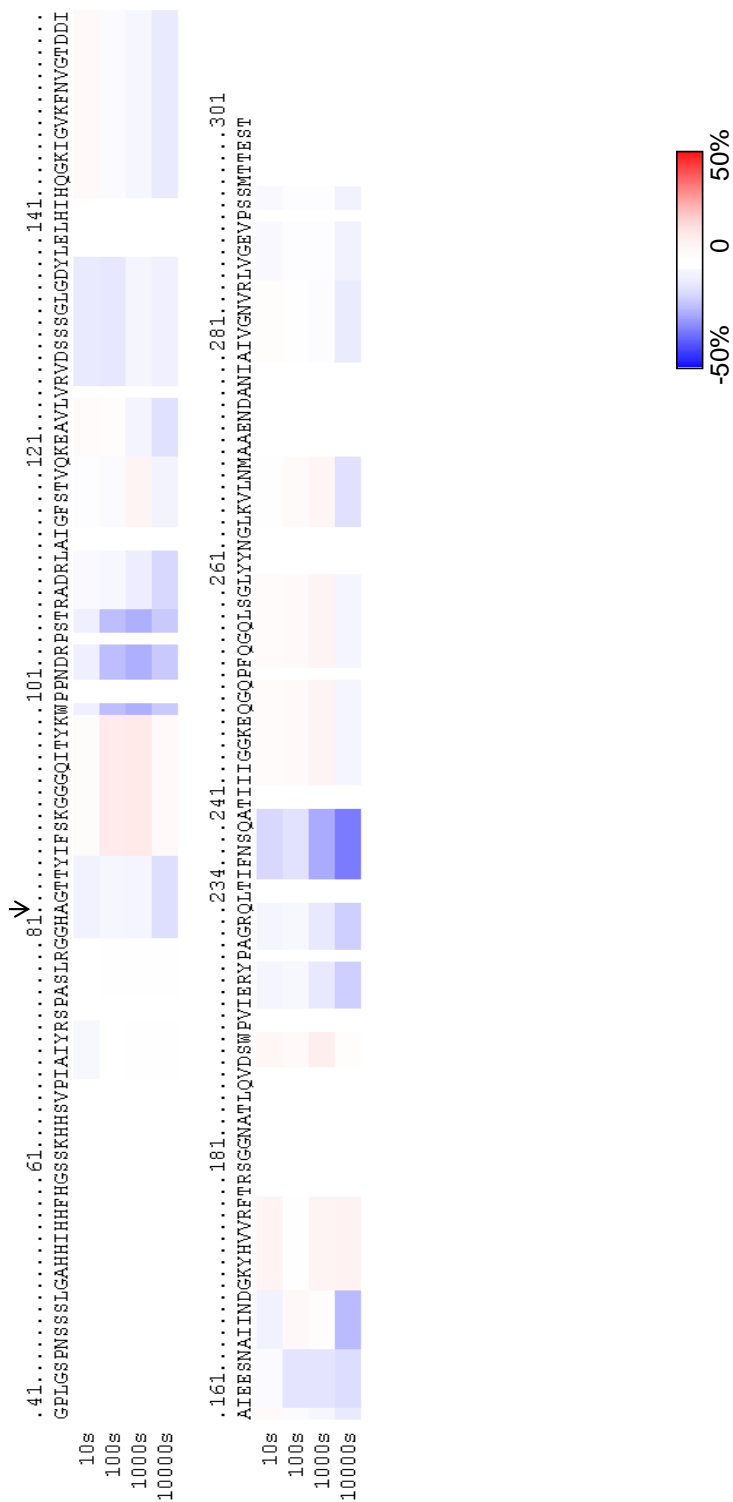


Figure 10a: Functional deuteration exchange profile for calcium enriched Neuroligin4. As with figures 6 & 8, deuteration profiles are displayed under the amino acid sequence. β denotes amino acids which take part in binding interactions with LNS 6 on α -neurexin1 and β -neurexin1 as a whole. Subsequent figures follow suit.

Ribbon Map of Neuroligin alone (Ca, in D%, Deuteration Level)

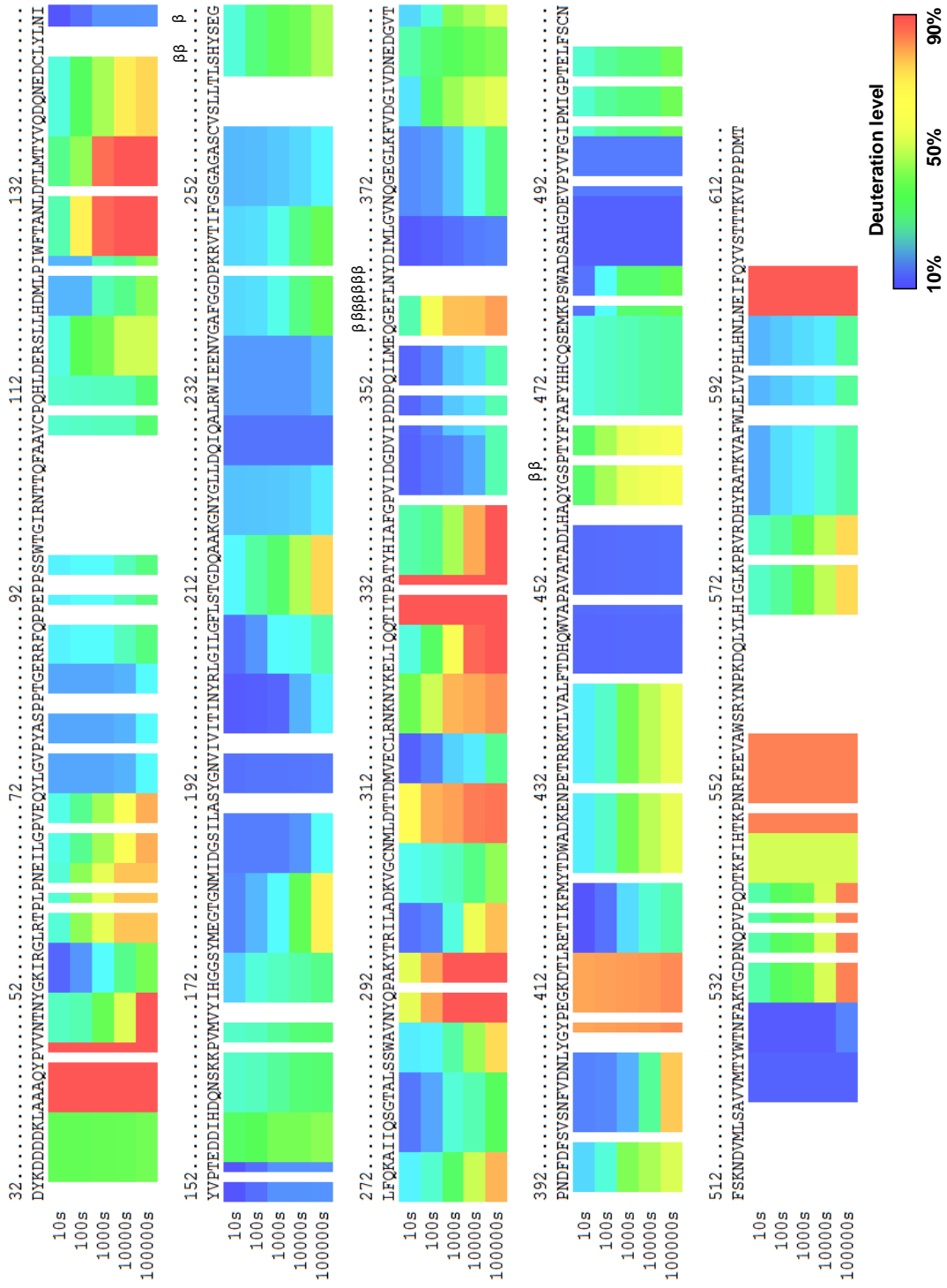


Figure 10b: Functional deuteration exchange profile for Neuroligin4: α -Neurexin1 complex at 1:1.2 mole ratio.

Ribbon Map of Neuroilgin in Complex with Alpha Neurexin (1:1.2, Ca, in D%, Deuteration Level)

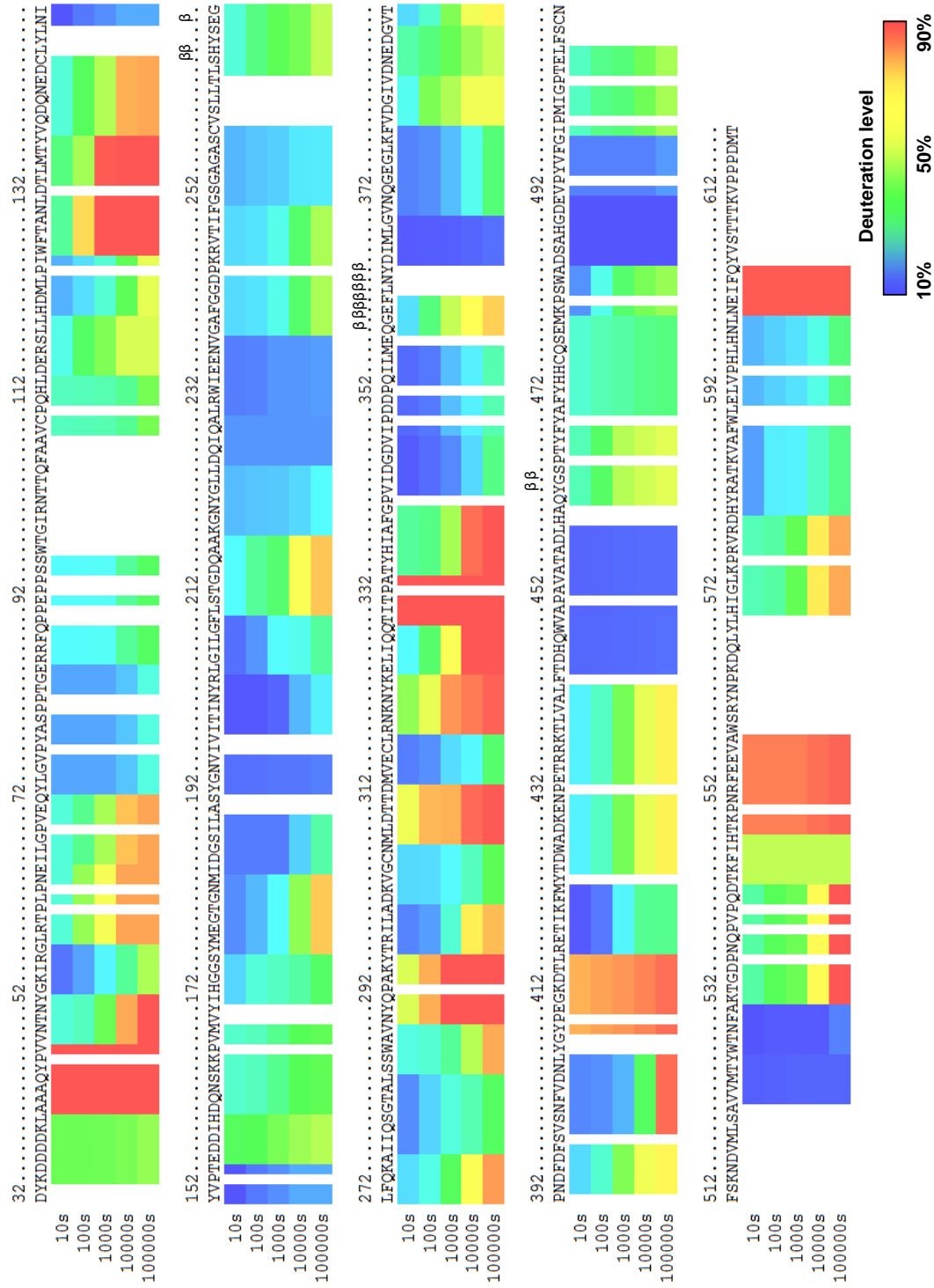


Figure 10c: Functional deuteration exchange profile for Neuroligin4:β-Neurexin1 complex at 1:1.2 mole ratio.

Ribbon Map of Neuroligin in Complex with Beta Neurexin (1:1.2 Ca, in D%, Deuteration Level)

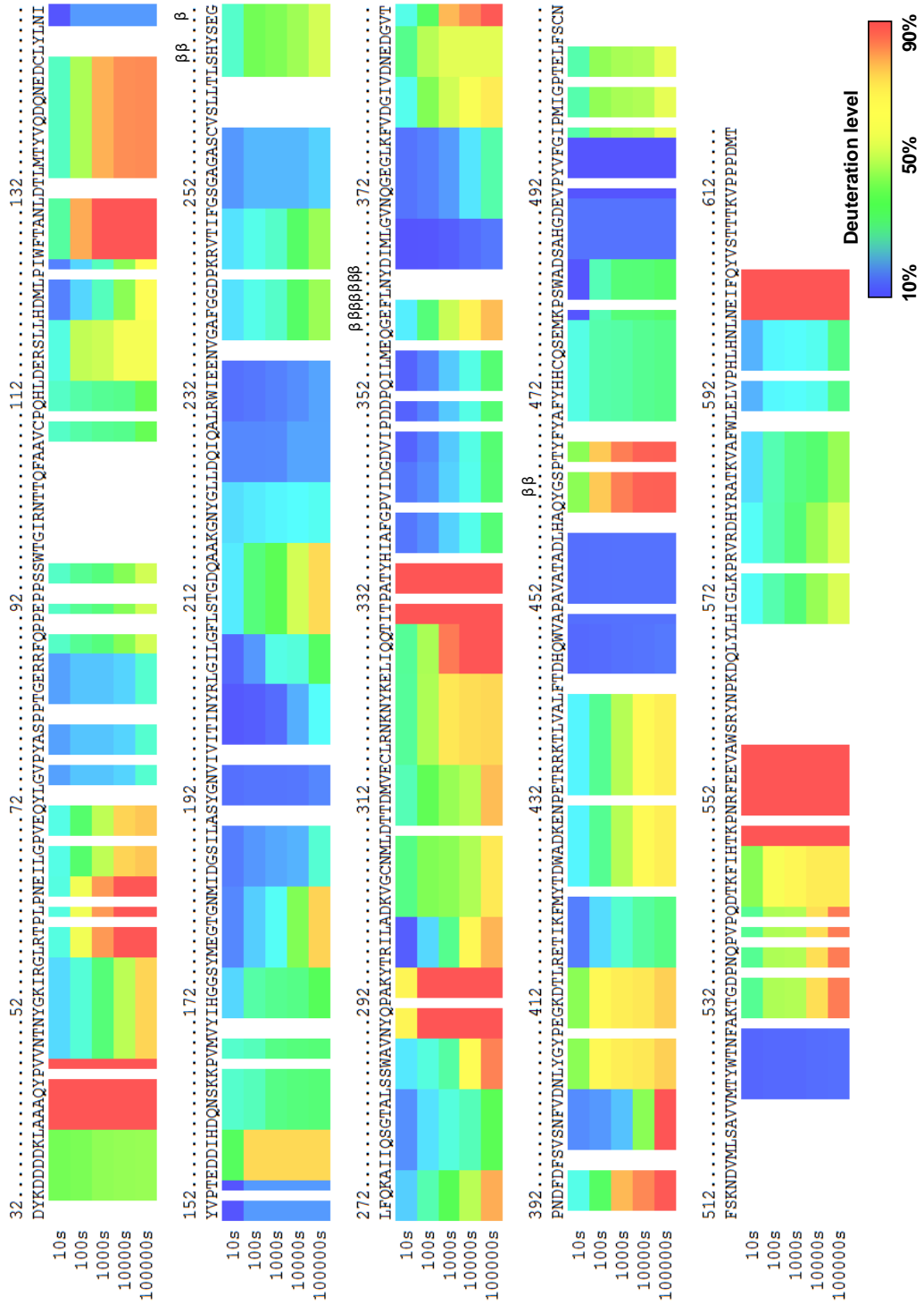


Figure 11a: Functional deuteration exchange difference map for Neuroligin4 calcium enriched and Neuroligin4: α -Neurexin 1:1.2 mole ratio. Calcium enriched deuteration levels are subtracted from 1:1.2 mole ratio deuteration levels. β denotes amino acids which take part in binding interactions with LNS 6 on α -neurexin1 and β -neurexin1 as a whole. Subsequent figures follow suit.

Neurologin in Alpha Complex (Ca) MINUS Neurologin Alone (Ca) (in D%, Deuteration Level)

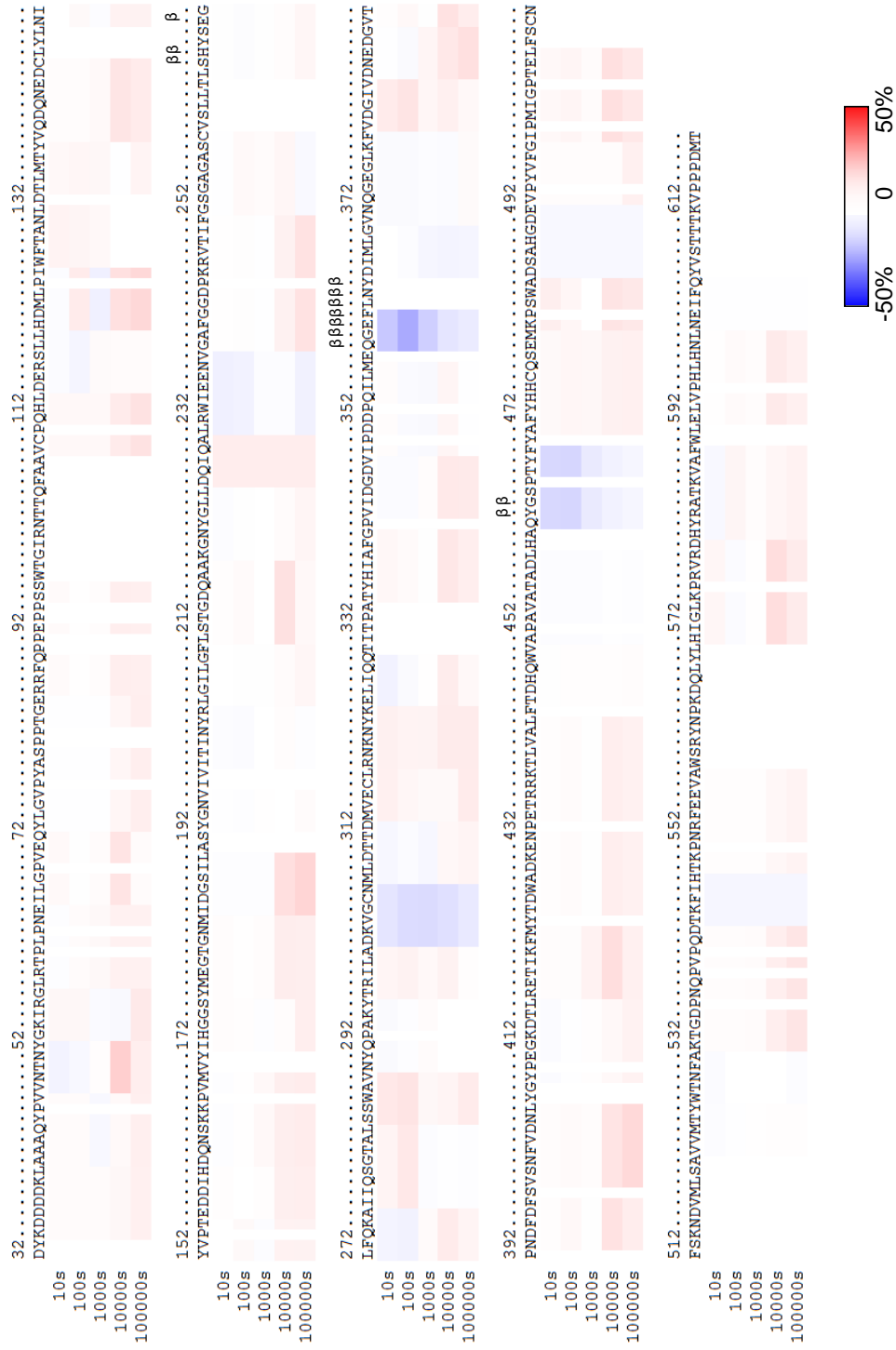


Figure 11b: Functional deuteration exchange difference map for Neuroligin4 calcium enriched and Neuroligin4:β-Neurexin 1:1.2 mole ratio. Calcium enriched deuteration levels are subtracted from 1:1.2 mole ratio deuteration levels.

Neurologlin in Beta Complex (Ca) MINUS Neurologlin Alone (Ca) (in D%, Deuteration Level)

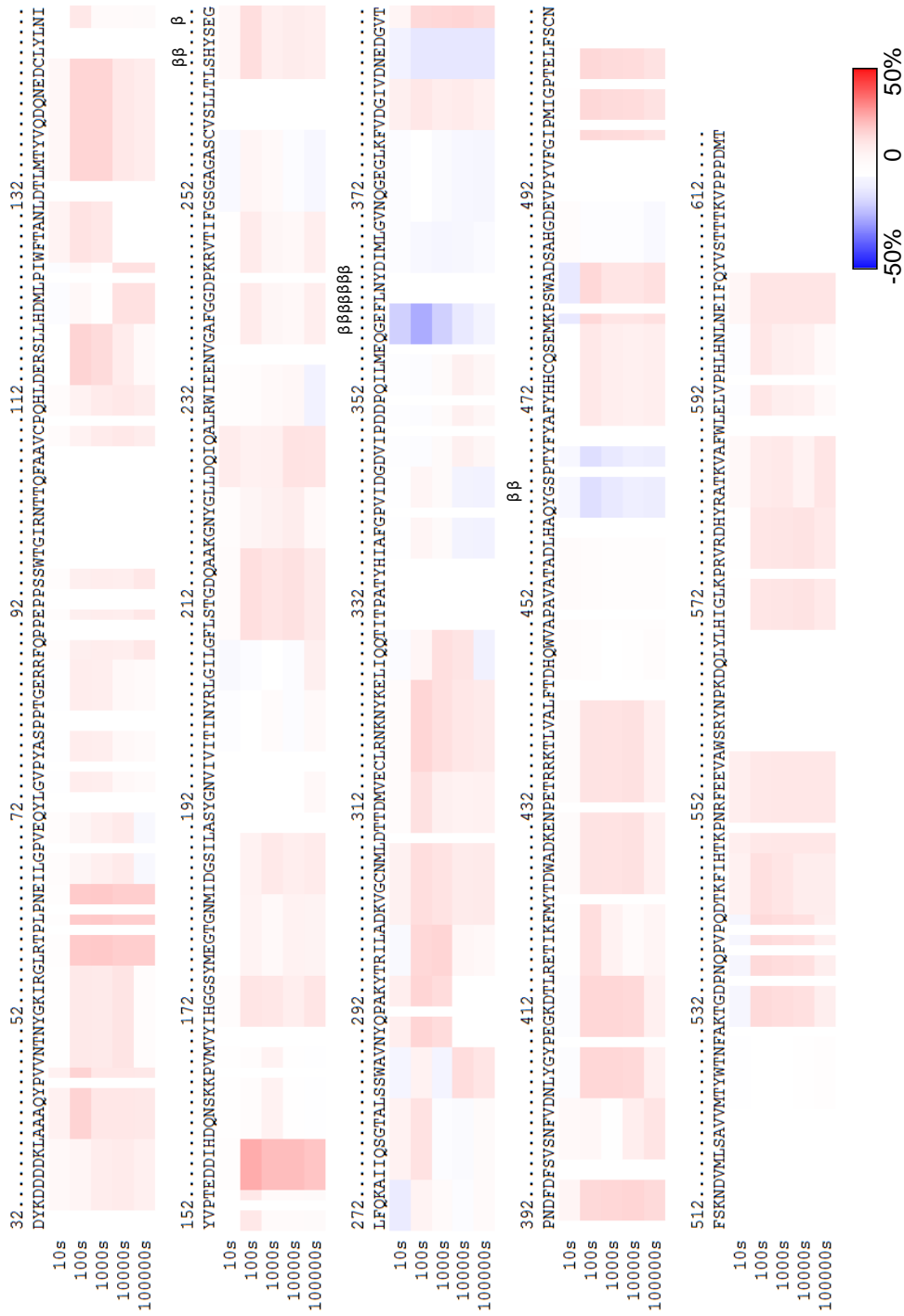
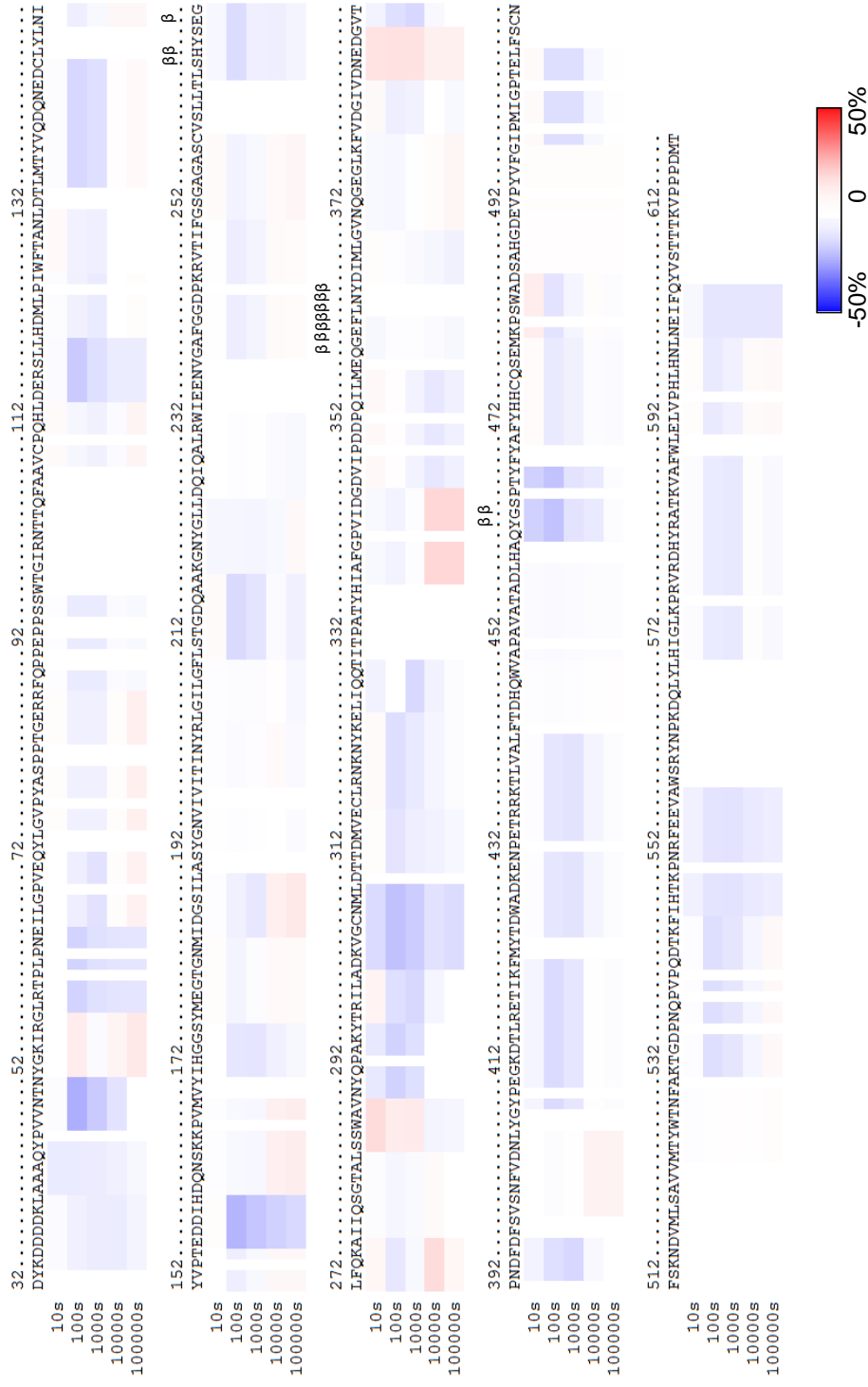


Figure 11c: Functional deuteration exchange difference map for Neuroligin4: α -Neurexin 1:1.2 mole ratio and Neuroligin4: β -Neurexin1 1:1.2 mole ratio. Neuroligin4: β -Neurexin1 deuteration levels are subtracted from Neuroligin4: α -Neurexin1 1:1.2 mole ratio deuteration levels.

Neurologin in Alpha Complex (Ca) MINUS Neurologin in Beta Complex (Ca) (in D%, Deuteration Level)



TABLES

Table 1: Coverage statistics for α -Neurexin1. Quench solution comprised 6.4 M GuHCl, 1 M TCEP, 0.8% formic acid, and 16.6% glycerol along with diluent solution of 0 M GuHCl, 0.8% formic acid and 16.6% glycerol.

α -NX1	Calcium Deficient	Calcium Enriched	1:1.2 mole ratio α -NX1:NL4	1:3 mole ratio α -NX1:NL4
LNS 4	83%	83%	83%	82%
LNS 5	77%	77%	77%	58%
EGF 3	0%	0%	0%	39%
LNS 6	76%	76%	76%	73%
Complete Protein	75%	77%	75%	70%
Total # Peptides	303	319	233	150

Table 2: Coverage statistics for β -Neurexin1. Quench solution comprised 6.4 M GuHCl, 1 M TCEP, 0.8% formic acid, and 16.6% glycerol along with diluent solution of 0 M GuHCl, 0.8% formic acid and 16.6% glycerol.

β -NX1	Calcium Deficient	Calcium Enriched	1:1.2 mole ratio β - NX1:NL4
% coverage	93%	95%	92%
Total # Peptides	215	233	166

Table 3: Coverage statistics for Neuroligin4. Quench solution comprised 6.4 M GuHCl, 1 M TCEP, 0.8% formic acid, and 16.6% glycerol along with diluent solution of 0 M GuHCl, 0.8% formic acid and 16.6% glycerol.

NL4	Calcium Deficient	Calcium Enriched	1:1.2 mole ratio NL4:α-NX1	1:1.2 mole ratio NL4:β-NX1
% coverage	73%	82%	82%	82%
Total # Peptides	422	422	364	308

REFERENCES

- Aiyegbo MS, Sapparapu G, Spiller BW, Eli IM, Williams DR, Kim R, Lee DE, Liu T, Li S, Woods VL Jr., Nannemann DP, Meiler J, Stewart PL, Crowe JE Jr. (2013) Human Rotavirus VP6-Specific Antibodies Mediate Intracellular Neutralization by Binding to a Quaternary Structure in the Transcriptional Pore. *PLoS One*. 8(5):e61101
- Arac D, Boucard AA, Ozkan E, Strop P, Newell E, SudhofTC, Brunger AT. (2007) Structures of neuroligin-1 and the neuroligin-1/neurexin-1 β complex reveal specific protein-protein and protein-Ca²⁺ interactions. *Neuron*. 56(6):992-1003.
- Arons MH, Thynne CJ, Grabrucker AM, Li D, Schoen M, Cheyne JE, Boeckers TM, Montgomery JM, Garner CC. (2012) Autism-associated mutations in ProSAP2/Shank3 impair synaptic transmission and neurexin-neuroligin-mediated transsynaptic signaling. *The Journal of Neuroscience*. 32(43):14966-78.
- Auld, V.J., Fetter, R.D., Broadie, K., and Goodman, C.S. (1995). Gliotactin, a novel transmembrane protein on peripheral glia, is required to form the blood-nerve barrier in *Drosophila*. *Cell*. 81, 757–767.
- Bai Y, Milne JS, Mayne L, Englander SW. (1993). Primary structure effects on peptide group hydrogen exchange. *Proteins: Structure, Function, and Genetics*. 17:75-86.
- Bollinger MF, Frei K, Winterhalter KH, Gloor SM. (2001) Identification of a novel neuroligin in humans which binds to PSD-95 and has widespread expression. *Biochemical Journal*. 356(Pt 2):581-8.
- Brose N. (1999) Synaptic cell adhesion proteins and synaptogenesis in the mammalian central nervous system. *Naturwissenschaften*. 86(11):516-24.
- Chandak MS., Nakamura T., Makabe K., Takenaka T., Mukaiyama A., Chaudhuri TK., Kato K, Kuwajima K. (2013) The H/D-Exchange Kinetics of the Escherichia coli Co-Chaperonin GroES Studied by 2D NMR and DMSO-Quenched Exchange Methods. *Journal of Molecular Biology*. S0022-2836(16)00239-8.
- Chen, X., Liu, H., Shim, A.H., Focia, P.J., and He, X. (2008). Structural basis for synaptic adhesion mediated by neuroligin-neurexin interactions. *Nature Structural and Molecular Biology*. 15, 50–56.
- Chung KY, Rasmussen SG, Liu T, DeVree BT, Chae PS, Calinski D, Kobilka BK, Woods VL Jr, Sunhara RK (2011) Conformational changes in the G protein Gs induced by the β 2 adrenergic receptor. *Nature*. 477(7366):611-5.
- Colby DW. & Prusiner SB. (2011) De novo generation of prion strains. *Nature reviews, Microbiology*. 9(11):771-7

- Comoletti, D., Flynn, R., Jennings, L.L., Chubykin, A., Matsumura, T., Hasegawa, H., Sudhof, T.C., and Taylor, P. (2003). Characterization of the interaction of a recombinant soluble neuroligin-1 with neurexin-1 β . *J. Biol. Chem.* 278, 50497–50505.
- Comoletti, D., De Jaco, A., Jennings, L.L., Flynn, R.E., Gaietta, G., Tsigelny, I., Ellisman, M.H., and Taylor, P. (2004). The Arg451Cysneuroligin-3 mutation associated with autism reveals a defect in protein processing. *The Journal of Neuroscience.* 24, 4889–4893.
- Comoletti, D., Flynn, R.E., Boucard, A.A., Demeler, B., Schirf, V., Shi J., Jennings, L.L., Newlin, H.R., Sudhof, T.C., and Taylor, P. (2006). Gene selection, alternative splicing, and post-translational processing regulate neuroligin selectivity for β -neurexins. *Biochemistry.* 45,12816–12827.
- Comoletti D, Grishaev A, Whitten AE, Tsigelny I, Taylo P, Trehella J. (2007) Synaptic arrangement of the neuroligin/ β -neurexin complex revealed by X-ray and neutron scattering. *Structure.* 15(6):693-705.
- Comoletti D, Miller MT, Jeffries CM, Wilson J, Demeler B, Taylor P, Trehella J, Nakagawa T. (2010) The macromolecular architecture of extracellular domain of α NRXN1: domain organization, flexibility, and insights into trans-synaptic disposition. *Structure.* 18(8):1044-523.
- Craig AM, Kang Y. (2007) Neurexin-neuroligin signaling in synapse development. *Current Opinion in Neurobiology.* 17(1):43-52.
- Cygler, M., Schrag, J.D., Sussman, J.L., Harel, M., Silman, I., Gentry, M.K., and Doctor, B.P. (1993). Relationship between sequence conservation and three-dimensional structure in a large family of esterases, lipases, and related proteins. *Protein Sci.* 2, 366–382.
- Davletov BA, Krasnoperov V, Hata Y, Petrenko AG, Sudhof TC. (1995) High affinity binding of α -latrotoxin to recombinant neurexin 1 α . *The Journal of Biological Chemistry.* 270(41):23903-5.
- Dean C, Scholl FG, Choih J, DeMaria S, Berger J, Isacoff E, Scheiffele P. (2003) Neurexin mediates the assembly of presynaptic terminals. *Nature Neuroscience.* 6(7):708-16.
- De Jaco A, Lin MZ, Dubi N, Comoletti D, Miller MT, Camp S, Ellisman M, Butko MT, Tsien RY, Taylor P. (2010) Neuroligin trafficking deficiencies arising from mutations in the α/β -hydrolase fold protein family. *The Journal of Biological Chemistry.* 285(37):28674-82.

- De Jaco A, Dubi N, Camp S, Taylor P. (2012) Congenital hypothyroidism mutations affect common folding and trafficking in the α/β -hydrolase fold proteins. *The FEBS journal*. 279(43):4293-305.
- de la Escalera, S., Bockamp, E.O., Moya, F., Piovant, M., and Jimenez, F. (1990). Characterization and gene cloning of neurotactin, a Drosophila transmembrane protein related to cholinesterases. *EMBO J*. 9, 3593–3601.
- Dyson HJ, Wright PE. (2004). Unfolded proteins and protein folding studied by NMR. *Chemical Reviews*. 104(8):3607-3622.
- Englander JJ, Del Mar C, Li W, Englander SW, Kim JS, Stranz DD, Hamuro Y, Woods VL Jr. (2003) Protein structure change studied by hydrogen-deuterium exchange, functional labeling, and mass spectrometry. *Proc. Natl. Acad. Sci. USA*. 100(12):7057-62
- Englander SW, Kallenbach NR. (1983). Hydrogen exchange and structural dynamics of proteins and nucleic acids. *Quarterly Review of Biophysics*. 16(4):521-655.
- Englander SW, Sosnick TR, Englander JJ, Mayne L. (1996). Mechanisms and uses of hydrogen exchange. *Current Opinion in Structural Biology*. 6:18-23.
- Fabrichny IP, Leone P, Sulzenbacher G, Comoletti D, Miller MT, Taylor P, Bourne Y, Marchot P. (2007) Structural analysis of the synaptic protein neuroligin and its β -neurexin complex: determinants for folding and cell adhesion. *Neuron*. 56(6):979-91
- Feng, J., Schroer, R., Yan, J., Song, W., Yang, C., Bockholt, A., Cook, E.H., Jr., Skinner, C., Schwartz, C.E., and Sommer, S.S. (2006). High frequency of neurexin 1 β signal peptide structural variants in patients with autism. *Neuroscience Letters*. 409, 10–13.
- Garcia RA, Pantazatos DP, Gessner CR, Go KV, Woods VL Jr, Villarreal FJ. (2005). Molecular interaction between matrilysin and the matrix metalloproteinase inhibitor doxycycline investigated by deuterium exchange mass spectrometry. *Molecular Pharmacology*. 64(4), 1128-1136.
- Garner CC, Zhai RG, Gundelfinger ED, Ziv NE. (2002) Molecular mechanisms of CNS synaptogenesis. *Trends in Neuroscience*. 25(5):243-51
- Glessner, J.T., Wang, K., Cai, G., Korvatska, O., Kim, C.E., Wood, S., Zhang, H., Estes, A., Brune, C.W., Bradfield, J.P., Imielinski M., Frackelton EC., Reichert J., Crawford EL., Munson J., Sleiman PM., Chiavacci R., Annaiah K., Thomas K., Hou C., Glaberson W., Flory J., Otieno F., Garris M., Soorya L., Klei L., Piven J., Meyer KJ., Anagnostou E., Sakurai T., Game RM., Rud DS., Zurawiecki D., McDougle CJ., Davis LK., Miller J., Posey DJ., Michaels S., Kolevzon A., Silverman JM., Bernier R., Levy SE., Schultz RT., Dawson G., Owley T., McMahon WM., Wassink TH., Sweeney JA., Nurnberger JI,

Coon H., Sutcliffe JS., Minshew NJ., Grant SF., Bucan M., Cook EH., Buxbaum JD., Devlin B., Schellenberg GD., Hakonarson H. (2009). Autism genome-wide copy number variation reveals ubiquitin and neuronal genes. *Nature*. 459, 569–573.

Hamuro Y, Coales SJ, Southern MR, Nemeth-Cawley JF, Stranz DD, Griffin PR. (2003) Rapid analysis of protein structure and dynamics by hydrogen/deuterium exchange mass spectrometry. *Journal of Biomolecular Techniques*. 14(3):171-82

Hlubek MD, Stuenkel EL, Krasnoperov VG, Petrenko AG, Holz RW. (2000) Calcium-independent receptor for α -latrotoxin and neurexin 1 α facilitate toxin-induced channel formation: evidence that channel formation results from tethering of toxin to membrane. *Molecular Pharmacology*. 54(3):519-28

Hsu S, Kim Y, Li S, Durrant ES, Pace RM, Woods VL Jr, Gentry MS. (2009) Structural insights into glucan phosphatase dynamics using amide hydrogen-deuterium exchange mass spectrometry. *Biochemistry*. 48(41):9891-902

Ichtchenko K, Nguyen T, Sudhof TC (1996) Structures, alternative splicing, and neurexin binding of multiple neuroligins. *The Journal of Biological Chemistry*. 271(5):2676-82

Jamain S, Quach H, Bncur C, Rastam M, Colineaux C, Gillberg IC, Soderstrom H, Giros B, Leboyer M, Gillberg C, Bourgeron T, Paris Autism Research International Sibpair Study. (2003) Mutations of the X-linked genes encoding neuroligins NLGN3 and NLGN4 are associated with autism. *Nature Genetics*. 34(1):27-9

Kaltashov IA, Eyles SJ. (2002). Studies of biomolecular conformations and conformational dynamics by mass spectrometry. *Mass Spectrometry Reviews*. 21(1):37-71.

Kim, H.G., Kishikawa, S., Higgins, A.W., Seong, I.S., Donovan, D.J., Shen, Y., Lally, E., Weiss, L.A., Najm, J., Kutsche, K., Descartes M., Holt L., Braddock S., Troxell R., Kaplan L., Volkmar F., Klin A., Tsatsanis K., Harris DJ., Noens I., Pauls DL., Daly MJ., MacDonald ME., Morton CC., Quade BJ., Guslla JF. (2008). Disruption of neurexin1 associated with autism spectrum disorder. *The American Journal of Human Genetics*. 82, 199–207

Lee JH, Li S, Liu T, Hsu S, Kim C, Woods VL Jr, Casteel DE. (2011) The amino terminus of cGMP-dependent protein kinase I β increases the dynamics of the protein's cGMP-binding pockets. *International Journal of Mass Spectrometry*. 302(1-3):44-52

Leone P, Comoletti D, Ferracci G, Conrod S, Garcia SU, Taylor P, Bourne Y, Marchot P. (2010) Structural insights into the exquisite selectivity of neurexin/neuroligin synaptic interactions. *The EMBO Journal*. 29(14):2461-71

- Liberski PP. (2012) Historical Overview of Prion Diseases: A View from Afar. *Folia Neuropathologica*. 50(1):1-12
- Maier CS, Deinzer ML. (2005). Protein conformations, interactions, and H/D exchange. *Methods in Enzymology*. 402:312-360.
- Miller MT, Mileni M, Comoletti D, Stevens RC, Harel M, Taylor P. (2011) The crystal structure of the α -neurexin-1 extracellular region reveals a hinge point for mediating synaptic adhesion and function. *Structure*. 19(6):767-78
- Missler M, Zhang W, Rohlmann A, Kattenstroth G, Hammer RE, Gottmann K, Sudhof TC. (2003) A-neurexins couple Ca²⁺ channel to synaptic vesicle exocytosis. *Nature*. 423(6943):939-48
- Morgan CR, Engen JR. (2009). Investigating solution-phase protein structure and dynamics by hydrogen exchange mass spectrometry. *Current Protocols in Protein Science*. 58(17.16):1-17
- Ollis, D.L., Cheah, E., Cygler, M., Dijkstra, B., Frolow, F., Franken, S.M., Harel, M., Remington, S.J., Silman, I., Schrag, J., Sussman J.L., Verschueren K.H.G., Goldman A. (1992). The alpha/beta hydrolase fold. *Protein Eng*. 5, 197–211.
- Olson, P.F., Fessler, L.I., Nelson, R.E., Sterne, R.E., Campbell, A.G., and Fessler, J.H. (1990). Glutactin, a novel Drosophila basement membrane-related glycoprotein with sequence similarity to serine esterases. *The EMBO Journal*. 9, 1219–1227.
- Prusiner SB, Groth DF, Bolton DC, Kent SB, Hood LE. (1984) Purification and structural studies of a major scrapie prion protein. *Cell*. 38(1):127-34
- Rudenko G, Nguyen T, Chelliah Y, Sudhof TC, Deisenhofer J. (1999) The structure of the ligand-binding domain of neurexin I β : regulation of LNS domain function by alternative splicing. *Cell*. 99(1):93-101
- Rujescu, D., Ingason, A., Cichon, S., Pietilainen, O.P., Barnes, M.R., Touloupoulou, T., Picchioni, M., Vassos, E., Ettinger, U., Bramon, E., Murray R., Ruggeri M., Tosato S., Bonetto C., Steinberg S., Sigurdsson E., Sigmundsson T., Petursson H., Gylfason A., Olason PI., Hardarsson G., Jonsdottir GA., Gustafsson O., Fossdal R., Giegling I., Moller HJ., Hartmann AM., Hofman P., Crombie C., Fraser G., Walker N., Lonngvist J., Suvisaari J., Tuulio-Henriksson A., Djurovic S., Melle I., Andreassen OA., Hansen T., Werge T., Kiemeny LA., Franke B., Veltman J., Buizer-Voskamp JE., GROUP Investigators, Sabatti C., Ophoff RA., Rietschel M., Nothen MM., Stefansson K., Peltonen L., St Clair D., Stefansson H., Collier DA. (2009). Disruption of the neurexin 1 gene is associated with schizophrenia. *Human Molecular Genetics*. 18, 988–996.

- Schapitz IU, Behrend B, Pechmann Y, Lappe-Siefke C, Kneussel SJ, Wallace KE, Stempel AV, Buck F, Grant SC, Schweizer M, Schmitz D, Schwarz JR, Holzbaur EL, Kneussel M. (2010) Neuroligin 1 is dynamically exchanged at postsynaptic sites. *The Journal of Neuroscience*. 30(38):12733-44
- Schumacher, M., Camp, S., Maulet, Y., Newton, M., MacPhee-Quigley, K., Taylor, S.S., Friedmann, T., and Taylor, P. (1986). Primary structure of *Torpedo californica* acetylcholinesterase deduced from its cDNA sequence. *Nature* 319, 407–409.
- Sebat J, Lakshmi B, Malhotra D, Troge J, Lese-Martin C, Walsh T, Yamrom B, Yoon S, Krasnitz A, Kendall J, Leotta A., Pai D., Zhang R., Lee YH., Hicks J., Spence SJ., Lee AT., Puura K., Lehtimaki T., Ledbetter D., Gregersen PK., Bregman J., Sutcliffe JS., Jobanputra V., Chung W., Warburton D., King MC., Skuse D., Geschwind DH., Gilliam TC., Ye K., Wigler M. (2007) Strong association of de novo copy number mutations with autism. *Science*. 2007
- Sharma S, Zheng H, Huang YJ, Ertekin A, Hamuro Y, Rossi P, Tejero R, Acton TB, Xiao R, Jiang M, Zhao L, Ma LC, Swapna GV, Aramini JM, Montelione GT. (2009) Construct optimization for protein NMR structure analysis using amide hydrogen/deuterium exchange mass spectrometry. *Proteins*. 76(4):882-94
- Sheckler LR, Henry L, Sugita S, Sudhof TC, Rudenko G. (2006) Crystal structure of the second LNS/LG domain from neuroligin 1 α : Ca²⁺ binding and the effects of alternative splicing. *The Journal of Biological Chemistry*. 281(32): 22896-905
- Spraggon G, Pantazatos D, Klock HE, Wilson IA, Woods VL Jr, Lesley SA. (2004) On the use of DXMS to produce more crystallizable proteins: structures of the T. maritime proteins TM0160 and TM 1171. *Protein science*. 13(12):3187-99
- Song, J.Y., Ichtchenko, K., Sudhof, T.C., and Brose, N. (1999). Neuroligin 1 is a postsynaptic cell-adhesion molecule of excitatory synapses. *Proc. Natl. Acad. Sci. USA* 96, 1100–1105.
- Sudhof TC. (2001) A-Latrotoxin and its receptors: neurexins and CIRL/latrophilins. *Annual Review of Neuroscience*. 24:933-62
- Sudhof TC. (2008) Neuroligins and neurexins link synaptic function to cognitive disease. *Nature*. 455(7215):903-11
- Szatmari, P., Paterson, A.D., Zwaigenbaum, L., Roberts, W., Brian, J., Liu, X.Q., Vincent, J.B., Skaug, J.L., Thompson, A.P., Senman, L., Feuk L., Qian C., Bryson SE., Jones MB., Marshal CR., Scherer SW., Vieland VJ., Bartlett C., Manqin LV., Goedken R., Segre A., Pericak-Vance MA., Cuccaro ML., Gilbert JR., Wright HH., Abramson RK., Betancur C., Bourgeron T., Gillberg C., Leboyer M., Buxbaum JD., Davis KL Hollander E, Silverman JM, Hallmayer J, Lotspeich L, Sutcliffe JS, Haines JL, Folstein SE, Piven J, Wassink TH,

Sheffield V, Geschwind DH, Bucan M, Brown WT, Cantor RM, Constantino JN, Gilliam TC, Herbert M, Lajonchere C, Ledbetter DH, Lese-Martin C, Miller J, Nelson S, Samango-Sprouse CA, Spence S, State M, Tanzi RE, Coon H, Dawson G, Devlin B, Estes A, Flodman P, Klei L, McMahon WM, Minshew N, Munson J, Korvatska E, Rodier PM, Schellenberg GD, Smith M, Spence MA, Stodgell C, Tepper PG, Wijsman EM, Yu CE, Rogé B, Mantoulan C, Wittmeyer K, Poustka A, Felder B, Klauck SM, Schuster C, Poustka F, Bölte S, Feineis-Matthews S, Herbrecht E, Schmötzer G, Tsiantis J, Papanikolaou K, Maestrini E, Bacchelli E, Blasi F, Carone S, Toma C, Van Engeland H, de Jonge M, Kemner C, Koop F, Langemeijer M, Hijmans C, Staal WG, Baird G, Bolton PF, Rutter ML, Weisblatt E, Green J, Aldred C, Wilkinson JA, Pickles A, Le Couteur A, Berney T, McConachie H, Bailey AJ, Francis K, Honeyman G, Hutchinson A, Parr JR, Wallace S, Monaco AP, Barnby G, Kobayashi K, Lamb JA, Sousa I, Sykes N, Cook EH, Guter SJ, Leventhal BL, Salt J, Lord C, Corsello C, Hus V, Weeks DE, Volkmar F, Tauber M, Fombonne E, Shih A, Meyer KJ. (2007). Mapping autism risk loci using genetic linkage and chromosomal rearrangements. *Nat. Genet.* 39, 319–328.

Tanaka H, Nogi T, Yasi N, Iwasaki K, Takaqi J. (2011) Structural Basis for Variant-Specific Neuroligin-Binding by α -Neurexin. *PLoS One.* 6(4):e19411

Tsutsui Y, Wintrode PL. (2007). Hydrogen/deuterium exchange-mass spectrometry: a powerful tool for probing protein structure, dynamics and interactions. *Current Medicinal Chemistry*; 14:2344-2358.

Ullrich B, Ushkaryov YA, Sudhof TC (1995) Cartography of neurexins: more than 1000 isoforms generated by alternative splicing and expressed in distinct subsets of neurons. *Neuron.* 14(3):497-507

Ushkaryov, Y.A., Petrenko, A.G., Geppert, M., and Sudhof, T.C. (1992) Neurexins: synaptic cell surface proteins related to the α -latrotoxin receptor and laminin. *Science* 257, 50–56.

Ushkaryov, Y.A., Hata, Y., Ichtchenko, K., Moomaw, C., Afendis, S., Slaughter, C.A., and Sudhof, T.C. (1994). Conserved domain structure of β -neurexins. Unusual cleaved signal sequences in receptor-like neuronal cell-surface proteins. *Journal of Biological Chemistry.* 269, 11987–11992.

Ushkaryov YA, Rohou A, Sugita S. (2008) A-Latrotoxin and its receptors. *Handbook of Experimental Pharmacology.* (184):171-206

Van Renterghem C, Iborra C, Martin-Moutot N, Lelianova V, Ushkaryov Y, Seagar M. (2000) A-latrotoxin forms calcium-permeable membrane pores via interactions with latrophilin or neurexin. *European Journal of Neuroscience.* 12(11):3953-62

Varoqueaux, F., Jamain, S., and Brose, N. (2004). Neuroligin 2 is exclusively localized to inhibitory synapses. *European Journal of Cell Biology.* 83, 449–456.

- Volynski KE, Menier FA, Lelianova VG, Dudina EE, Volkova TM, Rahman MA, Manser C, Grishin EV, Dolly JO, Ashley RH, Ushkaryov YA. (2000) Latrophilin, neurexin, and their signaling-deficient mutants facilitate α -latrotoxin insertion into membranes but are not involved in pore formation. *Journal of Biological Chemistry*. 275(52):41175-83
- Wales TE, Engen, JR. (2006). Hydrogen exchange mass spectrometry for the analysis of protein dynamics. *Mass Spectrometry Reviews*. 25(1), 158-170.
- Westfield GH, Rasmussen SG, Su M, Dutta S, DeVree BT, Chung KY, Calinski D, Velez-Ruiz G, Oleskie AN, Pardon E, Chae PS, Liu T, Li S, Woods VL Jr, Stevaert J, Kolbilka BK, Sunahara RK, Skiniotis G. (2011) Structural flexibility of the G α s α -helical domain in the β 2-adrenoceptor Gs complex. *Proc. Natl. Acad. Sci. USA*. 108(38):16086-91
- Wintrade PL, Friedrich KL, Vierling E, Smith JB, Smith DL. (2003). Solution structure and dynamics of a heat shock protein assembly probed by hydrogen exchange and mass spectrometry. *Biochemistry*. 42:10667-10673.
- Wintrade PL, Tsutsui Y. (2007). Hydrogen/deuterium exchange and mass spectrometry: a powerful tool for probing protein structure, dynamics and interactions. *Current Medicinal Chemistry*. 14:2344-2358.
- Yan J, Noltner K, Feng J, Li W, Schroer R, Skinner C, Zeng W, Schwartz CE, Sommer SS. (2008) Neurexin 1 α structural variants associated with autism. *Neuroscience Letters*. 438(3):368-70
- Zahir, F.R., Baross, A., Delaney, A.D., Eydoux, P., Fernandes, N.D., Pugh, T., Marra, M.A., and Friedman, J.M. (2008). A patient with vertebral, cognitive and behavioral abnormalities and a de novo deletion of NRXN1 α . *Journal of Medical Genetics*. 45, 239–243.
- Zhang AP, Bornholdt A, Liu T, Abelson DM, Lee DE, Li S, Woods VL Jr, Saphire EO. (2012) The ebola virus interferon antagonist VP24 directly binds STAT1 and has a novel, pyramidal fold. *PloS Pathogens*. 8(2):e1002550
- Zhang C., Milunsky JM., Newton S., Ko J., Zhao G., Maher TA., Tager-Flusberg H., Bolliger MF., Carter AS., Boucard AA., Powell CM., Sudhof TC. (2009) A neuroligin-4 missense mutation associated with autism impairs neuroligin-4 folding and endoplasmic reticulum export. *The Journal of Neuroscience*. 29(35):10843-54
- Zhang Q., Wang J., Li A., Liu H., Zhang W., Cui X., Wang K. (2013) Expression of neurexin and neuroligin in the enteric nervous system and their down-regulated expression levels in Hirschsprung disease. *Molecular Biology Reports* 40(4):2969-75

Zhang, W., Rohlmann, A., Sargsyan, V., Aramuni, G., Hammer, R.E., Sudhof, T.C., and Missler, M. (2005). Extracellular domains of α -neurexins participate in regulating synaptic transmission by selectively affecting N- and P/Q-type Ca²⁺ channels. *Journal of Neuroscience*. 25, 4330–4342.

Zhang Z., Smith DL. (1993). Determination of amide exchange by mass spectrometry: A new tool for protein structure elucidation. *Protein science*. 2:522-531.

Zweier, C., de Jong, E.K., Zweier, M., Orrico, A., Ousager, L.B., Collins, A.L., Bijlsma, E.K., Oortveld, M.A., Ekici, A.B., Reis, A., Schenck A., Rauch A. (2009). CNTNAP2 and NRXN1 are mutated in autosomal-recessive Pitt-Hopkins-like mental retardation and determine the level of a common synaptic protein in *Drosophila*. *The American Journal of Human Genetics*. 85, 655–666